Available online at www.sciencedirect.com
ScienceDirect
Trans. Nonferrous Met. Soc. China 34(2024) 26−49
Transactions of Nonferrous Metals Society of China
www.tnmsc.cn

Recent progress in NiMo-based amorphous alloys for electrocatalytic hydrogen evolution reaction

Si-xuan ZHANG[1], Jin-zhao HUANG[1], Dian-jin DING[1], Jun TANG[1], Xiao-long DENG[2]

1. School of Physics and Technology, University of Jinan, Jinan 250022, China;
2. School of Mathematics and Physics, Anhui University of Technology, Ma'anshan 243032, China

Received 21 June 2022; accepted 27 October 2022

Abstract: Electrocatalytic water splitting to produce green hydrogen is one of the important ways to develop sustainable energy systems. Highly active, low-cost amorphous alloys composed of transition metals Ni and Mo are widely regarded as efficient catalysts for hydrogen production. The catalysts represented by nickel−molybdenum (NiMo)-based amorphous alloys are focused on, the synthesis methods of amorphous alloys and their applications in the field of catalysis are summarized, and the application of NiMo alloys, NiMo-based medium entropy alloys, and NiMo-based high-entropy alloys are described respectively in electrocatalytic hydrogen evolution reaction (HER). In a word, NiMo-based amorphous alloy catalysts exhibit excellent hydrogen evolution performance by solving key scientific and technical problems with a reasonable function-oriented design. Finally, five issues in terms of preparation technology, component regulation, nanoscale, electronic structure and catalytic mechanism are proposed. This gives a clue for the design, preparation, structure−activity relationship and catalytic mechanism of catalysts.
Key words: NiMo alloys; amorphous alloy; water electrolysis; hydrogen evolution reaction

1 Introduction

The global energy crisis and the environmental pollution problems caused by the extensive use of fossil fuels and nuclear fuels continue to ferment. Hydrogen energy as a clean energy and renewable energy carrier with zero carbon emissions is an effective way to solve this problem [1−4]. However, the process of producing hydrogen through reforming and cracking of fossil fuels will generate too much CO and CO_2 greenhouse gases, which will pollute the environment. Therefore, the search for environmentally friendly, easy to mass-produce and highly efficient hydrogen production technology is one of the current research hotspots and urgent problems to be solved. Hydrogen production by electrolysis of water based on large-scale consumption of renewable energy is expected to be one of the best options, which also contributes to the realization of the dual-carbon goal [5−8].

Water electrolysis consists of two half-reactions, including the hydrogen evolution reaction (HER) on the cathode surface and the oxygen evolution reaction (OER) on the anode surface [9]. According to the different membrane materials of electrolyzers, electrolytic water hydrogen production technologies can be divided into four types [10,11]: alkaline water electrolysis (AWE), proton exchange membrane (PEM) electrolysis, solid oxide electrolysis cell (SOEC) and anion exchange membrane (AEM) electrolysis. AWE (Fig. 1(a)) is the most mature technology for hydrogen production by electrolysis of water. It has rich experience in industrial application, but the problems of low operating current density, high energy consumption, difficulty in adapting to the

Corresponding author: Jin-zhao HUANG, E-mail: ss_huangjinzhao@ujn.edu.cn; Xiao-long DENG, E-mail: dengxl84@ahut.edu.cn
DOI: 10.1016/S1003-6326(23)66380-0

volatility of renewable energy, and difficulty in rapid startup and load changes remain to be resolved [13]. The advantages of PEM (Fig. 1(b)) lie in high operating current density, low energy consumption, fast start-up and load change, but the problem of high cost of precious metal catalysts remains to be resolved, and it is currently in the initial stage from research and development to large-scale commercialization [14]. The SOEC (Fig. 1(c)) has low energy consumption, but needs to work at high temperature, and it is still in the preliminary demonstration stage [15−17]. AEM (Fig. 1(d)), as a new water electrolysis technology, has the advantages of low cost, high efficiency and non-precious metal catalyst. But the process is not yet mature, and the catalytic activity and stability need to be improved. However, no matter which technology is adopted, it faces a key problem, that is, the high energy barrier of the cathodic hydrogen evolution reaction of water electrolysis. Catalysts are one of the most effective ways to solve this problem. During the reaction process, the catalyst can form active intermediates to significantly reduce the overpotential and increase the current density to improve the overall catalytic efficiency [19,20].

Among the reported catalysts, amorphous alloys have high electrocatalytic activity due to their excellent properties such as long-range disorder, short-range order, and high corrosion resistance as new catalysts for the hydrogen evolution reaction of water electrolysis. In recent years, a series of amorphous alloy catalysts for water electrolysis have emerged one after another. For example, Pt-based catalysts can effectively reduce the overpotential of HER and achieve high-efficiency water splitting. But the scarcity and high cost of precious metals are difficult to meet the needs of large-scale hydrogen production [21−23]. Among transition metals, nickel with small hydrogen adsorption free energy (ΔG_{H^*}) is widely regarded as a low-cost, high-performance HER candidate catalyst, but it suffers from the deactivation during alkaline water electrolysis [24]. This deactivation can be reduced by alloying nickel with transition metal Mo on the left side of the periodic table, resulting in higher electrocatalytic activity than pure nickel. At the same time, the

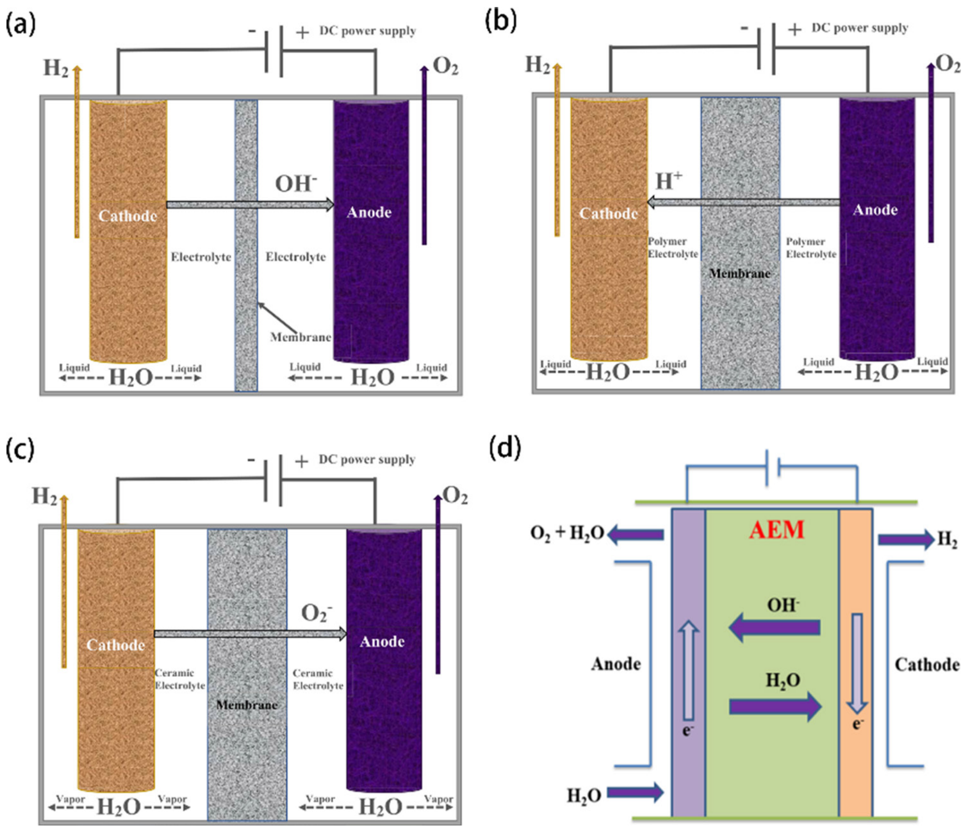

Fig. 1 Schematic diagrams of alkaline water electrolysis (AWE) [12] (a), proton exchange membrane (PEM) electrolysis [12] (b), solid oxide electrolysis cell (SOEC) [12] (c), and anion exchange membrane (AEM) electrolysis [18] (d)

excellent adsorption performance of Mo atoms for hydrogen makes NiMo amorphous alloys as one of the electrocatalysts with better HER activity in alkaline solution [25−28]. In addition, adding a third or more elements to NiMo binary alloy to form ternary and multi-elemental alloys are generally called medium-entropy alloys and high-entropy alloys. The addition of new elements and the synergistic effect between different atoms endow the high and medium entropy alloys (H/MEAs) with strong electrocatalytic performance [29,30].

In this review, we mainly summarize the electrocatalytic hydrogen evolution performance of NiMo-based amorphous alloy catalysts reported in recent years. The HER of NiMo alloys, NiMo-based medium-entropy alloys and NiMo-based high-entropy alloys in alkaline solution was introduced from the aspects of nanostructures, heterostructures, particles, supports and thin films on the catalytic performance. Finally, the problems to be solved for NiMo-based amorphous alloy catalysts were proposed and prospected.

2 Amorphous alloy

2.1 Overview of amorphous alloys

Amorphous alloy, also known as metallic glass, is a new type of amorphous materials in the 21st century. Amorphous alloys were first prepared in 1960 by Prof. DUWEZ using the melt rapid cooling method [31], and then various amorphous materials appeared one after another. Amorphous alloys have unique electronic and structural properties. In addition, high resistivity, strength, and hardness make them show relatively excellent soft magnetic properties [32] and mechanical properties. In the field of power electronics and the preparation of turbines materials, spring materials and cutting tools amorphous alloys have been applied [33]. Moreover, the long-range disorder and short-range order of the atomic arrangement of the amorphous alloy is its most notable feature [34,35], and this disorder makes the amorphous alloy in a highly unsaturated coordinate state and thus possesses more catalytic active centers to exhibit excellent catalytic performance.

2.2 Catalysis of amorphous alloys

It is well known that the catalytic activity of catalysts originates from crystal defects, and the presence of crystal defects in turn reduces the catalytic durability [36]. Unlike crystalline materials, amorphous alloy materials have no crystalline defects such as grain boundaries and dislocations [37], resulting in good corrosion resistance. At the same time, the atoms or the mixed arrangement of atoms in the amorphous alloy catalyst are disordered, and there is a synergistic effect between different atoms in the alloy. Density functional theory (DFT) calculations indicate that this synergistic effect is generally due to the change in electronic structure caused by the addition of atoms. Finally, the alloy has excellent electrocatalytic performance [38,39].

The long-range disordered and short-range ordered amorphous alloys make them widely used as catalysts in hydrogenation reaction, electrocatalytic hydrogen evolution reaction, electrocatalytic oxidation reaction, dehydrogenation reaction and ammonia synthesis reaction. In the 7th International Catalysis Conference held in the early 1980s, amorphous alloys were first proposed to be used in the field of catalysis [40]. Then, the research on amorphous alloy catalysts was mainly focused on hydrogenation reactions. Representative alloys include Ni−B and Ni−P [41]. In the past decades, the application of amorphous alloy catalysts in electrocatalytic oxidation reactions has attracted tremendous attention, especially the electrocatalytic oxidation of alcohols in fuel cells such as methanol, ethanol, and propanol. ZHENG's group has focused on Ni−B amorphous alloy nanoparticles [42−44], and pointed out that the electrocatalytic oxidation performance on small organic molecules (such as methanol, ethanol, and propanol) is higher than that of ordinary Ni metal. WU et al [45,46] studied Ni−B alloy for electrocatalytic methanol oxidation reaction. It is found that the doping of Co can change the electronic structure of nano-Ni−B, thereby enhancing the catalytic activity. In addition, the amorphous alloys are applied in electrocatalytic hydrogen evolution reaction in the full pH range. MA et al [47] demonstrated that the CoCrFeNiAl high-entropy alloy exhibited excellent HER performance in an acidic medium with an overpotential of only 73 mV. What's more, the Ni−Zr−Ti−Pt amorphous alloy with flexible honeycomb-like nanoporous sandwich structure prepared by surface dealloying showed excellent HER activity in alkaline medium with

Tafel slope as low as 30 mV/dec [48]. Amorphous alloy electrocatalysts show good electrocatalytic activity both in acidic and alkaline solutions [49].

2.3 Preparation methods of amorphous alloy

The preparation methods of amorphous alloys are mainly divided into three types: liquid quenching, physical vapor deposition (vacuum evaporation, sputtering, and ion plating) and chemical deposition (chemical vapor deposition, and liquid deposition).

The liquid quenching method is the earliest synthesis method of amorphous alloys [50]. The principle is to control the pressure of inert gas to spray the alloy liquid onto the roller, and then immediately cool down to form an amorphous alloy strip. The disadvantages of the catalyst prepared by this method are the small specific surface area and the complex and strict activation treatment before use, thus limiting its wide industrial application. Liquid quenching method also includes atomization, single rolling, dilution gas condensation, co-solvent water quenching and copper mold casting, among which atomization has high solidification rate and is one of the effective methods for preparing amorphous structure. Figure 2(a) shows a schematic diagram of gas atomization, and the principle is to disperse the liquid metal into tiny droplets by impinging the metal flow with a high-speed airflow, thereby achieving rapid solidification. The amorphous powder obtained by the atomization can be further used to prepare an amorphous coating, which has better wear resistance.

Physical vapor deposition (PVD) is mainly used to prepare films, including vacuum evaporation, sputtering and ion plating, among which sputtering is currently the most widely used [52−54]. The principle is to ionize the inert gas argon into argon ions under the action of a DC or radio frequency high-voltage electric field. Atoms disperse on the solid surface due to chemical bond breaking [55]. Figure 2(b) shows a schematic diagram of magnetron sputtering as a widely used technique for preparing alloy thin films, which can manufacture a multi-component alloy system by sputtering a variety of metal targets.

Chemical vapor deposition (CVD), including chemical vapor deposition and liquid deposition, is a process that applies gaseous substances to chemically react on solids and produce solid-state deposits (Fig. 2(c)), which can be used to prepare metal thin films and coatings. Liquid phase deposition (LPD) is a method for preparing amorphous thin films or particles using redox reactions in solution, including chemical reduction, electrochemical deposition, and electroless plating [58]. Among them, the electrodeposition is the most widely used preparation technology at

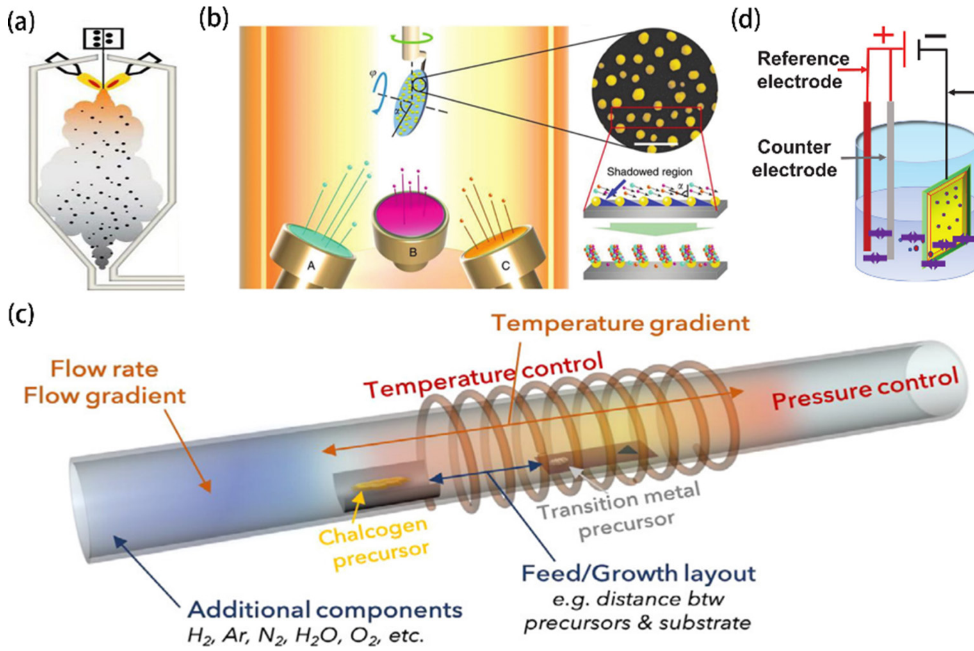

Fig. 2 Schematic diagrams of gas atomization [51] (a), magnetron sputtering [56] (b), chemical vapor deposition [57] (c), and electrodeposition [59] (d)

present, as shown in Fig. 2(d). It mainly uses the principle of electrochemistry to deposit metal, alloy or metal compound on a conductive substrate under the action of an electric field [60], usually accompanied by electron gain or loss. Through this technique, thin films with various functions can be obtained on the surface of the substrate. The electrodeposition method adjusts the film morphology by optimizing the electrodeposition conditions (including bath composition, additives, electrodeposition time and current density), and is a surface treatment technology with a long history and relatively mature technology.

There are many methods for the preparation of amorphous alloys, and each method has its own uniqueness and scope of application. For example, ion implantation, shock wave, and radiation can be used to obtain amorphous layered alloy materials [61]; on the other hand, solid-state reaction methods such as mechanical alloying, mechanical milling and mechanical deformation can produce amorphous alloy powder and thin films [62]. Furthermore, mechanical alloying has become an important method for the preparation of nanocomposites [63]. Although the approaches for amorphous alloys synthesis have always been a research hotspot in the material industry, more efficient and precise preparation methods are yet to be explored. It is believed that there will be major breakthroughs in the next few years.

3 Hydrogen evolution reaction of NiMo-based amorphous alloys

3.1 HER of NiMo alloys

High surface active area and high intrinsic electrocatalytic activity are the key factors for the selection of electrocatalytic materials. The remarkable characteristics of long-range disorder and short-range order in the atomic arrangement of amorphous materials make them in a highly coordinative unsaturated state and have more catalytically active sites, so they are good catalytic materials [64]. Due to the defects of poor catalytic activity and long-term instability in the medium of single-metal electrocatalysts, amorphous alloys composed of multiple elements have been widely studied as catalysts in the electrolysis of water. The amorphous alloy exhibits excellent electrocatalytic performance due to the element-to-element synergistic effect and its unique amorphous characteristics.

At present, among the transition metal Ni-based binary amorphous alloys, NiMo alloys are considered to be the best catalysts for electro-catalytic hydrogen evolution reaction, showing good catalytic activity in alkaline electrolytes. However, compared with Pt-based catalysts, the overpotential is still high and the overall efficiency is low, and thus the energy consumption is also high. Therefore, it is necessary to further improve the electrocatalytic activity of NiMo alloys. The commonly used methods are as follows: one is to modulate the electronic structure, and the other is to increase the specific surface area and expose more active sites. The above goals can be achieved by the rational design of catalyst composition, morphology and structural properties.

3.1.1 Nano-structure

Nanostructures usually include nanowires, nanorods, nanofibers, nanoribbons, porous, etc. The nanostructure of amorphous alloys enables them to have higher specific surface area and expose more active sites, which can overcome catalyst loss during catalysis. The shortcomings have also attracted great attention.

NiMo nanowires have been demonstrated to possess the outstanding electrocatalytic HER performance. HUANG et al [65] synthesized 1D NiMo nanowires by intercalating Li ions into $NiMoO_4$ nanorods using Li electrochemical tuning method. Electrochemical tests show that they have high HER activity in 1 mol/L KOH solution. This is mainly caused by the synergistic interaction between Ni and Mo, and the unique nanowire structure can expose more active sites, facilitating mass transfer and hydrogen bubble release. In addition, the difference in atomic radii in the solid solution leads to slight lattice distortion and compressive stress, which is beneficial to enhancing the electrocatalytic activity of HER. NAIRAN et al [66] prepared NiMo solid solution nanowire array electrodes by an aqueous solution synthesis method (Fig. 3(a)). After studying the two factors of Mo composition and growth temperature, it was found that $MoNi_4$ alloy electrode (1.60 at.% Mo) heated at 65 °C (denoted as NiMo-65) exhibits excellent catalytic performance (Fig. 3(b)), with a Tafel slope as low as 28 mV/dec (Fig. 3(c)). This excellent performance is attributed to lattice

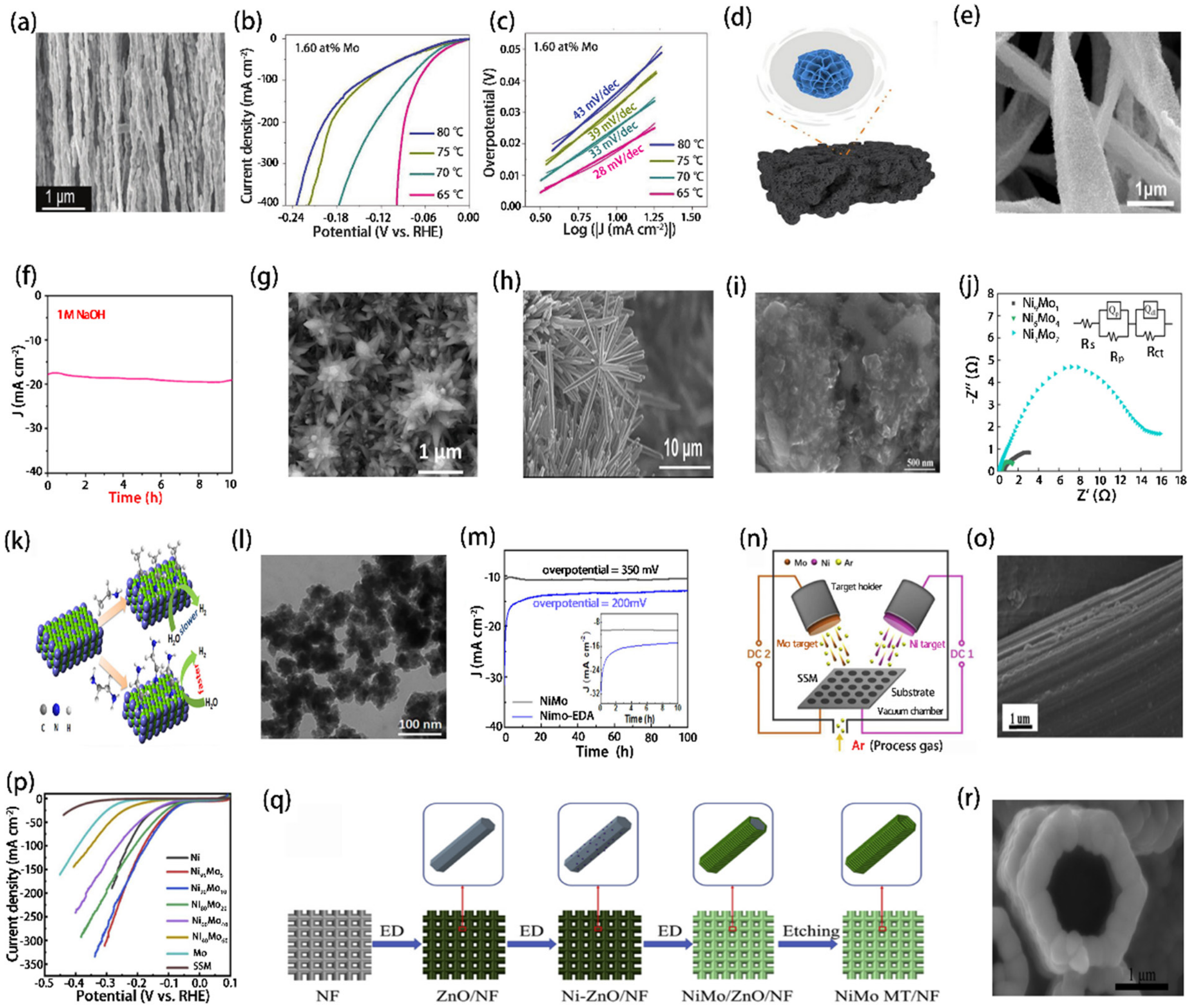

Fig. 3 SEM image of NiMo-65 electrode [66] (a); LSV curves of NiMo-electrode (1.60 at.% Mo) synthesized at different temperatures [66] (b); Corresponding Tafel plots [66] (c); Nano sponge NiMo solid solution [67] (d); TEM image of Ni_9Mo_1-PAH [68] (e); Chronoamperometric response at constant overpotential of 80 mV/s [68] (f); FESEM image of NiMo nanostar at EDA concentration of 200 g/L [69] (g); SEM image of ECT-NiMo/$NiMoO_4$ [71] (h); SEM image of Ni_6Mo_4 [72] (i); Nyquist plot of porous NiMo alloy in 1 mol/L KOH [72] (j); NiMo nanostructures with different amines and surface modification scheme of particles [76] (k); TEM image of NiMo-EDA [76] (l); Catalytic stability of NiMo and NiMo-EDA in 1 mol/L KOH (All measurements are in the absence of IR) [76] (m); Schematic diagram of method for preparing NiMo thin film catalysts by co-sputtering [77] (n); SEM image of $Ni_{90}Mo_{10}$ catalysts [77] (o); Tafel plot [77] (p); Schematic diagram of NiMo MT/NF preparation (Enlarged image on the NF sketch represents ZnO, NiZnO, NiMo/ZnO and NiMo MT) [88] (q); SEM image of NiMo MT/NF [88] (r)

distortion induced by Mo introduction, increased interfacial activity induced by alloy formation, and a large number of $MoNi_4$ active sites existing on the nanowire surface. SHANG et al [67] prepared NiMo nanoscale solid solution with 3D interconnected nanosponge structure. The large electrochemically active area (ECSA) (Fig. 3(d)), synergistic effect between Ni and Mo species, lattice distortion of solid solution and its high electrical conductivity result in excellent electrocatalytic activity and superior stability over a wide range of current densities in alkaline media as HER catalysts. The use of nanostructures to enhance the electrocatalytic performance of NiMo has been extensively investigated. For example, YANG et al [68] used electrospinning and in-situ vacuum reduction to construct a self-supporting, highly dispersed NiMo nanoribbon. The catalyst Ni_9Mo_1-PAH after heat treatment had a unique ribbon structure (Fig. 3(e)). This band structure has large active sites, which is favorable for electron transfer, and has sufficient mechanical strength. NiMo nanoribbons exhibit the HER activity in 1 mol/L KOH solution with an overpotential of 62 mV and a Tafel slope of 64 mV/dec at a current density of 10 mA/cm^2. The catalyst exhibits continuous HER activity at 80 mV/s after running for 10 h (about 3000 cycles), and the activity decay is minimal (Fig. 3(f)), indicating good stability.

In addition, some other nanostructured catalysts with unique morphology are also good candidates for HER. ZHANG et al [69] fabricated NiMo nanostar-structured electrodes by manipulating the variables of the electrochemical deposition process and changing the chemical composition, as shown in Fig. 3(g). The formation of nanostars increases the electrochemically active surface area, improves the inherent electrocatalytic activity, enhances the surface wettability, and avoids the use of binders in the electrode production process, resulting in strong HER electrocatalytic activity and durability. SAJJAD et al [70] synthesized $NiMoO_4$ by a hydrothermal annealing process, and then used a unique lithium-induced conversion reaction to convert $NiMoO_4$ into NiMo/$NiMoO_4$ nanorods (ECT-NiMo/$NiMo_4$), which exhibited relatively high performance in 1 mol/L KOH solution. ZHANG et al [71] prepared self-supporting one-dimensional Ni−Mo-based mixed-phase polyionic compounds by a simple and effective one-step molten salt method, and the SEM image (Fig. 3(h)) showed that the hierarchical structure formed by nanorod arrays was favorable for electrolyte and the bubbles migrated and exposed more active sites. Meanwhile, the modulation of Mo increases the electrochemically active area and modifies the surface electronic state of the catalyst, making the one-dimensional NiMo nanorods an excellent electrocatalyst for the electrocatalytic hydrogen evolution reaction.

In addition, the high specific surface area of the nanoporous structure is also an effective method to enlarge the catalytically active area of the material, which can achieve enhanced catalytic performance. XU et al [72] used microwave sintering powder metallurgy to prepare porous Ni_6Mo_4 electrocatalysts with stable performance and low overpotential. By analyzing the Nyquist plot (Fig. 3(j)), the R_{ct} value of the porous Ni_6Mo_4 alloy is much lower than that of other samples, indicating that the porous Ni_6Mo_4 alloy exhibits faster charge transfer efficiency. The nanoporous structure of the alloy can be clearly seen from the SEM image (Fig. 3(i)). This pore structure increases the specific surface area of the alloy, which is also the main reason for the high catalytic activity of Ni_6Mo_4. Catalysts with nanoporous structures have been demonstrated to enhance HER activity, and the effect of some controllable conditions on the electrocatalytic hydrogen evolution performance of porous NiMo alloys under alkaline conditions has been reported recently. BENAVENTE LLORENTE et al [73] investigated the effect of duty cycle in the range of 30%−70% on spherical NiMo alloys prepared by pulsed electrodeposition and showed that with decreasing duty cycle, the Mo content increased and the charge transfer resistance decreased. The change of alloy composition tuned the nanostructure-related electronic structure of the catalyst, so the alloy obtained at 30% duty cycle showed the highest HER activity in 1 mol/L KOH. ZU et al [74] successfully fabricated porous NiMo alloys with directional pore morphologies by freeze casting, and investigated the effect of pore orientations parallel and perpendicular to the H_2 overflow direction on the hydrogen evolution performance of NiMo alloys. It is found that the pores distributed in the porous NiMo alloy exhibit obvious anisotropy. The researchers verified that “parallel” sample has higher HER activity and faster electron transfer rate than “perpendicular” sample by performing linear sweep voltammetry and EIS in 6 mol/L KOH solution. This is attributed to the relatively larger active surface area of “parallel” sample, representing stronger electron transfer ability and greater hydrogen spillover rate. Besides, the introduction of oxygen vacancies can tune the electronic configuration and surface properties. ZHU et al [75] introduced oxygen vacancies for the electrocatalytic hydrogen evolution reaction of $Ni_{61}Zr_{36}Mo_3$ by dealloying, and the amorphous Ni−Mo−O nanoporous layer outside the sample structure gave it excellent HER performance in alkaline electrolytes.

In conclusion, adjusting the nanostructures (nanowires, nanorods, nanosheets, nanoporous, etc) to increase the specific surface area and the number of active sites is a favorable way to enhance the electrocatalytic activity of electrocatalysts.

3.1.2 Particle, film, heterostructure

(1) Particle

Particles are a relatively common form of NiMo-based catalysts. This catalyst has abundant active sites, which can enhance the electron transfer rate and enhance the electrocatalytic activity. As shown in Fig. 3(k), GAO et al [76] selected primary amines of EA and DDA and diamines of EDA, HDA and DDDA to modify the surface of NiMo catalysts, and ethylenediamine (EDA) modified NiMo (NiMo−EDA)) retained the original granular morphology, as shown in Fig. 3(l). The research shows that the prepared NiMo−EDA catalyst has high HER activity. Compared with unmodified NiMo, its overpotential is reduced to 268 mV, the Tafel slope is as low as 89 mV/dec, and the charge transfer resistance is also significantly decreased. Moreover, NiMo−EDA does not fluctuate significantly at overpotentials of 350 mV and 250 mV for 100 h (Fig. 3(m)). Therefore, ethylene-diamine significantly improves the HER activity of NiMo alloys by reducing the charge transfer resistance and adjusting the electronic structure of the interfacial active sites.

(2) Film

Films are another common form of NiMo-based catalysts. The dense surface structure enables them to have a large electrochemically active surface area (ECSA), which can effectively improve the catalytic activity of the catalyst. SUN et al [77] synthesized a series of NiMo alloy thin films by the composition gradient sputtering. Figure 3(n) shows the sputtering schematic diagram. Due to the synergistic effect between nickel and molybdenum, the intrinsic electrocatalytic activity of nickel−molybdenum alloy electrocatalysts is enhanced, resulting in excellent HER performance. It is shown that the element concentration does not affect the morphology and structure of the nickel−molybdenum alloy thin film (Fig. 3(o)). The electrochemical test in alkaline solution shows the performance of the $Ni_{90}Mo_{10}$ electrocatalyst by the LSV curves (Fig. 3(p)). The potential is significantly lower than that of Ni, Mo, and other concentrations of NiMo catalysts, showing better HER performance. YUAN et al [78] synthesized NiMo electrocatalysts by electrodeposition, and the thickness of the prepared catalyst film for HER is about 1 μm. This excellent structure enables it to exhibit good electrocatalytic activity and low Tafel slope, as tested for electrochemical stability in 1 mol/L KOH and 1 mol/L KOH + 0.5 mol/L NaCl at 10 mA/cm^2 galvanostatic current. It shows high stability and no obvious performance decay, and is a high-performance HER catalyst for water splitting. In addition, adjusting the surface structure of the catalyst film to a microporous structure is an effective method to improve the catalytic performance. YU et al [79] studied the porous NiMo films prepared by electrodeposition under hypergravity field, and the abundant pore structure uniformly distributed on the surface of the film made it have excellent electrocatalytic hydrogen evolution activity in alkaline solution. Due to the easy peeling phenomenon of the film, YUAN et al [80] obtained a NiMo film catalyst with strong adhesion and high thermal stability in the citrate−ammonia electrodeposition system by optimizing the pH value of the solution (pH=10). The dense film of NiMo with amorphous structure enables it to exhibit excellent HER performance in alkaline solution.

(3) Heterostructure

Metal nanoparticles or thin films combined with 2D materials can form heterostructures. Catalysts with this structure mainly optimize the electrocatalytic hydrogen evolution reaction by establishing electron transport channels between materials and adjusting the electronic structure of the catalyst [81,82]. Heterostructures have attracted much attention in recent years. Density functional theory (DFT) and density of states (DOS) calculations of catalyst can more clearly grasp the catalytic mechanism. The HER performance of metal−metal oxide and alloy−metal oxide heterostructures in alkaline media has been studied in recent years, especially the heterostructure electrocatalysts related to Ni and Mo. Recently, the $Ni_5Mo/NiCo_2O_4$ heterojunction prepared by CHEN et al [83] has excellent HER activity. The combination of Ni_5Mo and $NiCo_2O_4$ transfers electrons from Co^{2+}/Co^{3+} to Ni^0/Mo^0, optimizing the electronic structures of the active centers of Ni^0, Mo^0, and Co^{3+}, thereby greatly enhancing the intrinsic HER activity. In alkaline electrolyte, the overpotential is 44 mV at a current density of 10 mA/cm^2 for HER. Meanwhile, a stable current density of 10 mA/cm^2 can be achieved at a low cell voltage of 1.54 V, and the long-term stability can reach 50 h. The formation of nanostructures is often accompanied by construction of heterostructures, which greatly reduces the charge-transfer resistance of the catalysts and exposes more active sites, enabling the catalysts to have outstanding HER performance in alkaline media. For example, DENG et al [84] prepared Ni−MoO_2 heterostructured nanosheets by hydrothermal reduction, and the as-prepared electrodes only required an overpotential of 40 mV to reach a current density of 10 mA/cm^2 in alkaline media. WANG et al [85] prepared Ni−MoO_2 heterostructured nanosheets by a three-step method of electrochemical deposition, hydrothermal treatment, and calcination, which exhibited excellent electrocatalytic hydrogen evolution performance over a wide pH range. Density functional theory calculations show that the three-phase heterostructure has better electrocatalytic activity. QIAN et al [86] investigated nitrogen-doped carbon-coated Ni/MoO_2 nanoneedle with a three-phase heterostructure (Ni/MoO_2@CN), a three-phase heterojunction with high intrinsic activity and more active sites. The self-supporting nanoneedles with faster mass diffusion and bubble release make them have excellent bifunctional electrocatalysts in alkaline media. In addition, the smaller-sized Ni−MoO_2@SCG nanoparticle heterojunction has higher catalytic activity in alkaline solution [87].

The synergistic effect between heterostructures is one of the main reasons for efficient water splitting for hydrogen production. However, most of the current heterostructure catalysts are synthesized from two materials, and the heterostructures composed of more materials have not been deeply studied.

3.1.3 Carrier

Growing catalysts on carriers can effectively improve the electrocatalytic hydrogen evolution performance. Nickel foam (NF), copper foam (CF), carbon cloth, carbon nanotubes (CNTs), and reduced graphene oxide (rGO) are good supports, and their large specific surface area, high electrical conductivity, and pore structure can promote the rapid penetration of electrolytes and the rapid release of hydrogen bubbles during water electrolysis to enhance the HER performance of low-activity catalysts.

Using foamed nickel (NF) as a carrier, its pore structure and metal properties are favorable for metal electrodeposition. As shown in Fig. 3(q), CAO et al [88] prepared NiMo alloy microtubes radially arranged on NF (NiMo MT/NF) by electrodepositing NiMo nanoparticles on ZnO template and then removing the template. The microtubule structure can be clearly seen (Fig. 3(r)), and its abundant active sites and high surface area enable the alloy to exhibit efficient electron transport properties. Compared with nickel foam (NF), the NiMo MT/NF electrode possesses smaller overpotential and Tafel slope, mainly because the interaction between the foamed nickel substrate and the microtubule structure makes the NiMo MT/NF exhibit better catalytic activity and long-term stability. The corrosion resistance and high activity of nickel in alkaline electrolyzers make it a good choice for carrier. ABUIN et al [89] prepared and characterized several nickel−molybdenum coatings on nickel using DC and pulsed current electrodeposition, among which the best HER activity was obtained for the Ni−Mo/Ni alloy prepared by pulsed electroplating from a NF bath. The characterization of this Ni−Mo prepared on Ni substrates revealed an amorphous state with a rough cauliflower-like microstructure. Compared with nickel foam, copper foam has lower cost and higher electrical conductivity, but its electrocatalytic activity is lower and its corrosion resistance is poorer, which limits its wide application. Using chemical or electrochemical methods to generate $Cu(OH)_2$ nanowires on the surface of copper foam can effectively avoid the defects of pure CF. The NiMo/Cu nanowires (NM-CNWs) prepared by ZHAO et al [90] possess good water splitting performance and are excellent bifunctional electrocatalysts.

In addition, high specific surface area and good electrical conductivity enable graphene to serve as an electrocatalyst substrate to improve the activity of electrocatalytic hydrogen evolution reaction. SHETTY et al [91] added rGO to NiMo alloy to obtain Ni−Mo−rGO, which showed higher electrocatalytic activity and better stability. The researchers employed different techniques to explore the hydrogen evolution reaction mechanism and kinetics of the Ni−Mo−rGO composite electrode in 1 mol/L KOH solution, and characterized its surface morphology and chemical composition. The results show that the rGO-induced Ni−Mo alloy has better catalytic activity for hydrogen production compared with the binary alloy coating, due to graphene acting as an exchange platform to facilitate electron transfer and transport during HER. The enhanced HER performance of the Mo−rGO composite coating is also attributed to the high specific surface area and good electrical conductivity of graphene in the alloy matrix.

In addition to common materials such as nickel foam and graphene, metal materials such as stainless steel, gold, and silver are also good HER electrode carriers [92]. Single-metal nanomaterials are highly corrosive, as conductive substrates can produce synergistic effects with electrocatalysts. The three-dimensional conductive substrate formed by the combination of silver nanowires and polyurethane foam has been demonstrated to have good electrical conductivity and stability, which can help improve HER performance [93]. LIU et al [94] prepared a NiMo alloy (3D AgNWs@NiMo/PU) on a three-dimensional silver nanowire conductive substrate (3D AgNWs/PU) with excellent electro-catalytic hydrogen evolution performance. The good electrolyte permeability, abundant active sites, good electronic conductivity, and electro-catalytic synergy of 3D AgNWs/PU endow the 3D AgNWs@NiMo/PU electrode with high electrocatalytic activity. In addition, the 3D AgNWs@NiMo/PU electrode does not need to use a binder during the hydrogen evolution process, which can improve the hydrogen evolution performance and stability of the electrode. Due to the high cost of precious metal silver itself, its wide application is limited. In comparison, the earth-abundant stainless steel material costs less. GÓMEZ et al [95] obtained a NiMo coating with high corrosion resistance on the surface of 316L stainless steel by electrodeposition process. This material significantly reduces the cost of electrodes used in conventional alkaline electrolytic cells, and has good electrocatalytic hydrogen evolution performance.

In conclusion, the electronic configuration and exposure of more active sites through the design of catalyst composition and morphology, as well as the synergistic effect between metallic Ni and Mo can effectively improve the electrocatalyst activity for water splitting. Table 1 gives the HER performance of NiMo alloy catalysts in alkaline medium. In conclusion, whether the alloy is nanosized or designed into a three-dimensional structure as well as a particle and porous structure, the specific surface area of the catalyst is increased. Similarly, applying the catalyst on a suitable conductive substrate can effectively solve the defects of poor conductivity and insufficient specific surface area of the catalyst. These methods are all helpful to improve the HER performance of amorphous NiMo alloys. Certainly, an in-depth understanding of the interrelationship among morphology, composition, and electrocatalytic performance will facilitate the development of NiMo electrocatalysts.

3.2 HER of NiMo-based medium entropy alloys

Medium-entropy alloys (MEAs) composed of one or two elements added to binary alloys generally exhibit better electrocatalytic activity for HER. This is because the disordered distribution and unsaturated sites of the multi-elements in the medium-entropy alloy can effectively adjust the electronic structure and increase the specific surface area [96,97]. More importantly, the synergistic effect between different species is more beneficial to the electrocatalytic activity. This remarkable catalytic activity and long-term durability of medium-entropy alloys make them effective catalytic materials for HER. Recently, there have been many studies on the HER performance of medium-entropy alloys based on NiMo alloy. For example, adding a new transition metal to the alloy makes the transition metal with less filled d orbital form an alloy with the transition metal with more filled d orbital, resulting in a new synergistic effect. And by combining metal with metal phosphide or sulfide to improve hydrogen adsorption, etc., the obtained new catalysts all show good electro-catalytic hydrogen evolution performance.

3.2.1 Nanostructure

In nanostructured medium-entropy alloy, the synergistic effect between various elements, the large specific surface area of nanostructures, and the exposure of more active sites are the factors that affect the improvement of electrocatalytic activity.

Phosphating NiMo alloys is one of the effective methods to prepare the nanostructures. ZHANG et al [98] used a combination of EDM and phosphating to prepare Ni−Mo−P planar electrodes at different temperatures, and the sheet-like nanosheet structure could not only obtain a large specific surface area, but also expose more active sites. Moreover, the gap between the nanosheet

Table 1 HER properties of NiMo alloys

Catalyst	Electrolyte	Overpotential, η_{10}/mV	Tafel slope/(mV·dec^{-1})	Reference
NiMo nanowires	1 mol/L KOH	73	37.2	[65]
NiMo nanowire arrays	1 mol/L KOH	17	28	[66]
$Ni_{0.33}Mo_{0.67}$-900	1 mol/L KOH	37	39.2	[67]
Ni_9Mo_1-PAH nanoribbons	1 mol/L KOH	62	64	[68]
NiMo nanostar	1 mol/L KOH	60	87	[69]
ECT-NiMo/$NiMo_4$ nanostave	1 mol/L KOH	61	84	[70]
NiMonano stave	1 mol/L KOH	191.2 (η_{100})	78.8	[77]
Ni_6Mo_4 nanoporous	1 mol/L KOH	37	82.1	[72]
NiMo30％	1 mol/L KOH	180	124	[73]
NiMo nanoporous	6 mol/L KOH	137	94	[74]
NiMoO nanoporous	1 mol/L KOH	71±2.6 (η_{20})	57±3	[75]
NiMo-EDA	1 mol/L KOH	72	89	[76]
$Ni_{90}Mo_{10}$ film	1 mol/L KOH	58	91	[77]
NiMo film	1 mol/L KOH	36.8	33.6	[78]
NiMo porous film	1 mol/L KOH	47 (η_{100})	136.7	[79]
NiMo(pH10)	6 mol/L KOH	63.9	84	[80]
$Ni_5Mo/NiCo_2O_4$	1 mol/L KOH	44	60.9	[83]
Ni-MoO_2	1 mol/L KOH	40	116	[84]
MoO_2-Ni/CC	1 mol/L KOH	46	56.9	[85]
Ni/MoO_2@CN	1 mol/L KOH	33	45	[86]
$NiMoO_2$@SCG	1 mol/L KOH	79.97	53.3	[87]
NiMo MT/NF	1 mol/L KOH	119	119	[88]
NiMo/Ni	4.2 mol/L KOH	400 (η_{200})	133	[89]
NiMo/Cu	1 mol/L KOH	152 (η_{20})	107	[90]
AgNWs@NiMo/PU	1 mol/L KOH	32	72	[94]

arrays is conducive to the rapid mass transfer and rapid precipitation of the generated hydrogen, resulting in higher HER activity and better stability. The researchers also revealed that the $Ni_{12}P_5$ produced after phosphorylation has a smaller $|\Delta G_{H^*}|$ value than Ni_4Mo by density flooding theory calculations, confirming the effect of $Ni_{12}P_5$ on the electrocatalytic hydrogen precipitation performance of NiMoP. The rational design of nanoarray structures has been extensively studied, which can effectively improve the electrocatalytic hydrogen evolution performance by accelerating charge transfer, increasing specific surface area, and exposing more active sites. For example, as shown in Fig. 4(a), ZHANG et al [99] designed and fabricated oxygen-containing $NiMoP_2$ nanowire arrays by controlled partial phosphorylation of metal oxide precursors (Fig. 4(b)). The nanowire array provides a very ideal open hierarchical network for fast mass transfer in HER, increasing the reactive sites for the reaction, and the resulting O-$NiMoP_2$/Ni has excellent HER performance. Importantly, density flooding theory calculations showed that the addition of O atoms brought the Gibbs free energy (ΔG_{H^*}) of the catalyst closer to the optimal value (ΔG_{H^*}=0 eV) (Fig. 4(c)), enhancing the H adsorption on the $NiMoP_2$ surface and further improving the electrocatalytic hydrogen evolution performance.

Adding an appropriate amount of Co element to NiMo alloy to form nanostructured catalysts can also enhance the electrocatalytic performance. HU

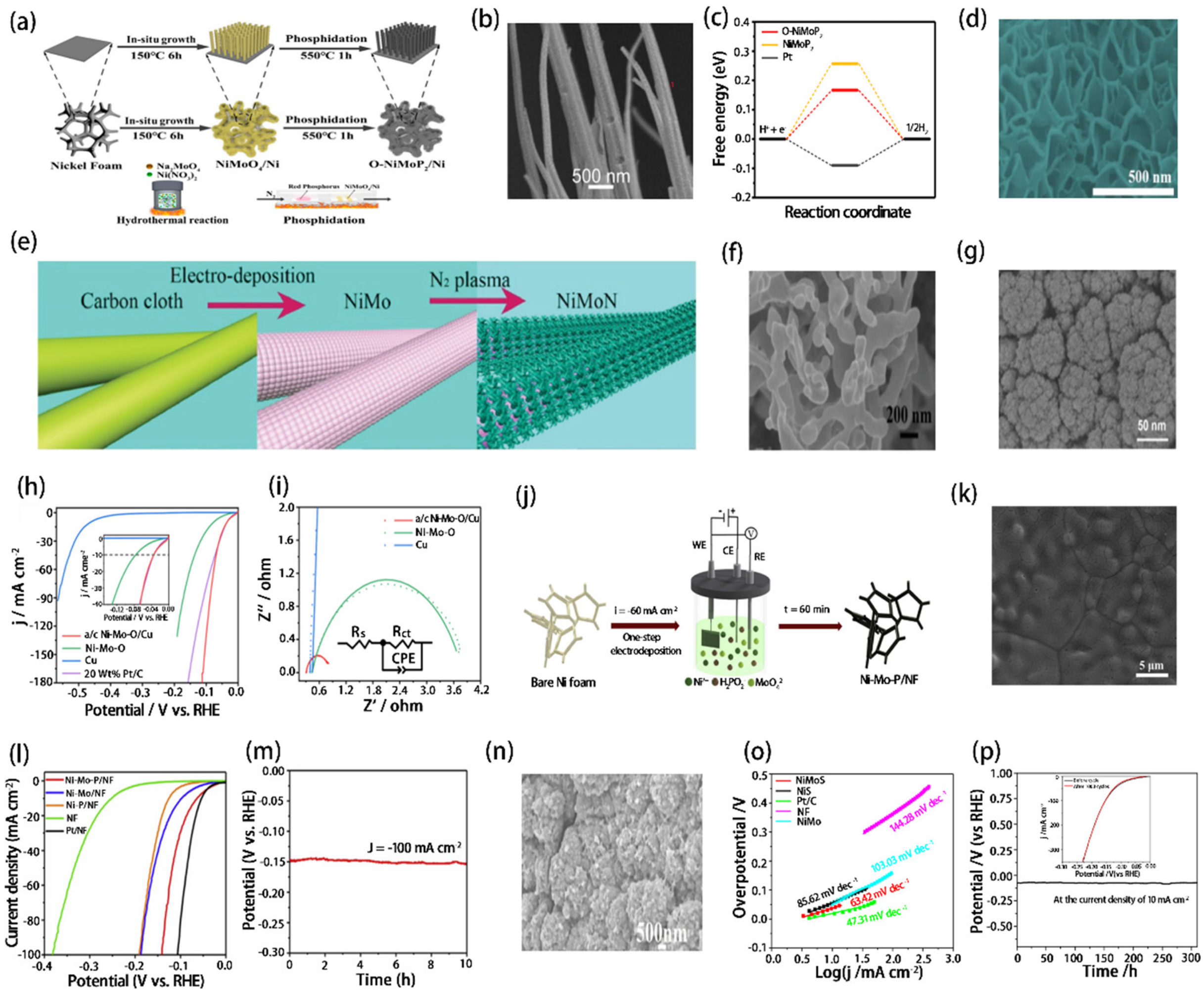

Fig. 4 Schematic of fabrication process of O−NiMoP$_2$/Ni [99] (a); SEM image of O-NiMoP$_2$/Ni [99] (b); Corresponding free-energy diagram for HER on NiMoP$_2$, O−NiMoP$_2$ surface, and Pt [99] (c); FESEM image of 3D flower-like structures of NiCoMo-LDH [100] (d); Schematic diagram of fabrication process of 3D hierarchical porous nickel−molybdenum nitride (NiMoN) [102] (e); SEM image of NiMoN [102] (f); FESEM image of a/c NiMoO/Cu [108] (g); Polarization curves of a/c NiMoO/Cu, NiMoO, Cu and 20 wt.% Pt/C [108] (h); Nyquist plot of a/c NiMoO/Cu, NiMoO, Cu and 20 wt.% Pt/C [108] (i); Schematic diagram of fabrication method of Ni−Mo−P/NF [109] (j); FESEM image of Ni−Mo−P/NF film [109] (k); Performance of various electrodes in line scan voltammogram [109] (l); Stability test results of Ni−Mo−P/NF at current density of 100 mA/cm^2 [109] (m); Low-magnification FESEM image of NiMoS/NF [114] (n); Tafel plot of NiMoS/NF [114] (o); Chronopotentiometry curve of NiMoS/NF electrode at 10 mA/cm^2 (Inset is LSV curve of NiMoS/NF electrode before and after 1000 cycles) [114] (p)

et al [101] proposed a transitional non-noble metal-based ternary NiMoCo hybrid nanowire array, the addition of Co enabled the Ni−Mo binary system to form a highly mixed chemically bound state, and the modulation occurred in the electronic structure. Compared with binary alloys, Co atoms in ternary alloys become the preferred catalytically active sites, thus making NiMoCo an efficient HER electrocatalyst. JEGHAN et al [100] used a one-pot hydrothermal method to prepare a flower-like three-dimensional hierarchical ternary nickel−cobalt layered double hydroxide (NiCoMo-LDH) without a substrate. It can be clearly seen from the SEM image (Fig. 4(d)) that the three-dimensional flower-like structure consists of many two-dimensional nanosheets. The nanosheet composition, which provides additional active sites for NiCoMo-LDH, coupled with the efficient incorporation of Ni, Co, and Mo in the layered structure, synergistic effect, and high electrochemical surface area, and finally enables NiCoMo-LDH to exhibit remarkable electrocatalytic activity, is an efficient electrocatalyst for HER. The CoNiMo alloy obtained through electrodeposition by LASZCZYŃSKA et al [103] also exhibited outstanding electrocatalytic hydrogen evolution performance in 1 mol/L KOH solution, mainly due to the nanocrystalline structure of the CoNiMo coating and the large surface area of the ternary deposits.

Designing the catalyst surface structure can increase the active surface area, thereby improving HER performance. For example, YAN et al [104] synthesized NiFeMoS anemone-like nanorods (NiFeMoS/NF-P) by the electrodeposition and hydrothermal vulcanization using polyether P123 and MoO_4^{2-} as morphology directing agents. The electrochemical tests show that NiFeMoS/NF-P as a bifunctional electrocatalyst exhibits excellent electrocatalytic performance in 1 mol/L KOH. Only an overpotential of 100 mV is required to reach a current density of 10 mA/cm^2 for HER and tafel slope as low as 121 mV/dec. The polarization curve of NiFeMoS/NF-P has no obvious change after 1000 CV cycles at a scan rate of 100 mV/s, showing good durability. The high activity of this catalyst is attributed to the anemone-like nanorod structure and high specific surface area. At the same time, this unique structure also enhances the synergistic effect between metals.

Porous structures can provide larger specific surface area and more active sites, and facilitate ion transport, thereby enhancing HER performance [105]. As shown in Fig. 4(e), ZHANG et al [102] treated NiMo alloy thin films with N_2 plasma and subsequently successfully fabricated 3D porous NiMoN electrocatalytic materials (Fig. 4(f)) and showed that the catalyst has low overpotential, Tafel slope in alkaline solution, and excellent durability at different current densities. The high catalytic performance of NiMoN is mainly attributed to its improved electronic/chemical properties and exposure of more active sites, which are mainly related to its unique porous structure. PANEK et al [106] prepared $Ni_{50}Mo_{40}Ti_{10}$ alloy by mechanical alloying and heat treatment, and the alloy after heat treatment showed high porosity and good electrocatalytic hydrogen evolution performance in alkaline environment. The reason for the enhanced activity of this material is the increased specific surface area of the catalyst and the high intrinsic activity of the catalyst, and Ti also has a positive effect on the electrochemical performance of the electrode.

3.2.2 Particle, film, heterostructure

(1) Particle

The introduction of Cu and Zn metals into NiMo alloys can easily form a cauliflower-like particle structure, and significantly promote the HER activity. XIA et al [107] prepared a NiMoCu alloy electrode with a cauliflower-like structure. The synergistic effect of the electrocatalytic components and the increased specific surface area of the cauliflower-like particle structure made the prepared electrode have lower overpotential, Tafel slope and better HER stability. Besides, YAO et al [108] synthesized amorphous/crystalline multiphase NiMoO/Cu (a/c NiMoO/Cu) as an efficient HER electrocatalyst by electrodeposition method. a/c NiMoO/Cu (Fig. 4(g)) consists of many cauliflower-shaped particles. The catalyst possesses good electrical conductivity, abundant interface, and efficient electron transfer rate, resulting in ultra-low overpotential (34.8 mV) and Tafel slope (38.7 mV/dec) (Figs. 3(h, i)). In addition, a/c NiMoO/Cu also exhibits outstanding stability and can homogeneously catalyze hydrogen evolution for 20 h. This high catalytic activity and stability of the a/c NiMoO/Cu electrode is mainly attributed to the enhanced electrical conductivity and redistribution of electron density by the introduction of metallic Cu, and amorphous Ni−Mo−O provides abundant active centers for HER. With the seamless connection between the center, Ni−Mo−O and Cu also guarantee the high electron transfer rate of the electrocatalyst, solving the problem of poor conductivity of amorphous materials.

(2) Film

At present, the deposition method is the most common method for preparing thin films, which can realize the construction of large-area amorphous alloy thin films with tunable composition. TOGHRAEI et al [109] successfully deposited a non-precious metal Ni−Mo−P ternary alloy thin film by one-step electrodeposition method (Fig. 4(k)), and the preparation process is schematically shown in Fig. 4(j). The catalyst exhibits an overpotential of only 63 mV (Fig. 4(l)) and a Tafel slope as low as 87.3 mV/dec at a current density of 10 mA/cm^2 in 1 mol/L KOH solution. And the catalyst exhibits excellent durability at a current density of 100 mA/cm^2 (Fig. 4(m)). The strong electrocatalytic performance of this electrode can be attributed to the synergistic effect of Ni, Mo, and P elements and their roles in changing the electronic structure of the catalyst. In addition, the network structure of the film provides a high electrochemical active area (ECSA) for HER, and because of this, the electrode does not require any nanostructure to enhance HER activity. BADRNEZHAD et al [110] prepared NiMoFe thin films by one-step electrodeposition as an efficient HER electrocatalyst. Overpotential of only 65 mV is required at a current density of 10 mA/cm^2. The addition of Fe element increases the electrocatalytic activity of HER, and the synergistic effect among nickel, molybdenum, and iron elements and the binder-free structure also make it have strong HER performance. ABHILASH et al [111] prepared NiMoP alloy coatings by chemical reduction. The synergistic effect of molybdenum, nickel and phosphorus in the coatings significantly enhanced the electrocatalytic activity of the coatings. The study of NiMoP has confirmed that the high specific surface area, more active sites, and excellent electrical conductivity of NiMoP coatings for accelerating electron transfer make them promising alternatives for noble metal-based electrocatalysts for water electrolysis. Furthermore, the presence of tungsten carbide nanoparticles and molybdenum content in NiMo/WC films enhances the actual surface area and intrinsic catalytic activity of the composites, with excellent electro-catalytic hydrogen evolution performance [112].

(3) Heterostructure

The heterostructures formed by the alloy nanoparticles and metal oxides have better catalytic performance than metal-metal oxide heterojunctions. LIU et al [113] prepared NiMoFe NPs@MoO_2 NPAs HER electrocatalysts by anchoring dense ternary NiMoFe alloy nanoparticles on hierarchical MoO_2 nanopillar arrays to greatly enrich the active centers. And the inherent high HER activity, as well as good charge and mass transport, make the catalyst have good catalytic activity and stability in alkaline solution.

3.2.3 Carrier

A good support can tune the electronic structure by increasing the number of active sites, facilitating charge transfer to the catalyst surface, and building connections with the catalyst to enhance the electrocatalytic hydrogen evolution performance.

Nickel foam has been widely used as a carrier in electrochemistry. For example, WANG et al [114] used a simple and controllable electrochemical deposition method to prepare nickel−molybdenum−sulfur amorphous microstructures on nickel foam (NiMoS/NF), and FESEM images showed that the surface had honeycomb shape (Fig. 4(n)). The as-prepared samples were electrochemically tested in alkaline solution. The as-deposited NiMoS/NF electrode exhibited excellent electrocatalytic activity for the hydrogen evolution reaction (HER). Only an overpotential of 37 mV is required to reach a current density of 10 mA/cm^2 in 1 mol/L KOH solution and the Tafel slope is as low as 63.42 mV/dec (Fig. 4(o)). It also exhibited an ultra-long durability of over 310 h at 10 mA/cm^2 (Fig. 4(p)). The excellent electrocatalytic activity is mainly attributed to the lower charge transfer resistance, large electrochemically active surface area (ECSA) and abundant microstructure of the as-deposited NiMoS/NF electrocatalyst. IM et al [115] deposited ZnNiMoPi directly on nickel foam (NF) by immersing the substrate in MoO_4^{2-} modified Zn phosphating bath at 80 °C for only 1 min, which has a relatively high HER activity and durability in 1 mol/L KOH solution.

Among many carbon material carriers, graphite carbon felt is an excellent choice. Its high electrical conductivity, chemical stability, and uniform pores can improve the durability and catalytic activity of electrocatalysts in alkaline solutions. Recently, ROS et al [116] fabricated highly efficient bifunctional catalysts for seawater splitting and proposed a regeneration method by immersing electrodes in acidified seawater to deal with salt deposition. They deposited nickel−molybdenum−iron trimetallic electrocatalysts on low-cost graphitic carbon felts for HER in seawater and alkaline seawater, and its performance was almost comparable to that of Ni−Mo.

It is easy to find that the addition of one or two elements into NiMo alloys has been extensively studied, and the synergistic effect between the elements promotes an increase in catalytic activity. The HER performance of NiMo-based medium-entropy alloy catalysts in alkaline medium is given in Table 2. At the same time, the structure, morphology and element ratio of the catalyst greatly affect the catalytic performance.

Table 2 HER performance of entropy alloys with NiMo matrix

Catalyst	Electrolyte	Overpotential, η_{10}/mV	Tafel slope/(mV·dec^{-1})	Reference
NiMoP nanosheets	1 mol/L KOH	276 (η_{100})	76.4	[98]
O−$NiMoP_2$/Ni	1 mol/L KOH	31	62.11	[99]
NiMoCo nanowire array	1 mol/L KOH	23	34	[100]
NiCoMo-LDH	1 mol/L KOH	93	51	[101]
NiFeMoS nano-stave	1 mol/L KOH	100	121	[103]
NiMoN porous materials	1 mol/L KOH	109	95	[105]
$Ni_{50}Mo_{40}Ti_{10}$ porous materials	5 mol/L KOH	300 (η_{100})	226	[106]
NiMoCu	6 mol/L KOH	105	200	[107]
a/c NiMoO/Cu	1 mol/L KOH	34.8	38.7	[108]
NiMoP film	1 mol/L KOH	63	87.3	[109]
NiMoFe film	1 mol/L KOH	65	63	[110]
NiMoP film	1 mol/L NaOH	128	101	[111]
NiMoFe NPs@MoO_2 NPAs	1 mol/L KOH	24	33	[113]
NiMoS/NF	1 mol/L KOH	37	63.42	[114]

3.3 HER of NiMo-based high-entropy alloys

The disordered distribution of atoms in high-entropy alloys composed of multiple elements and the wide compositional tuning range make them rich in defects and unsaturated sites for deep optimization of electronic structure, active sites, surface adsorption energies [117]. High-entropy alloys (HEAs) exhibit many unique properties due to the combined effects of high entropy, slow diffusion, lattice distortion, and the cocktail effect. For example, single solid solution structures (body-centered cubic, face-centered cubic, or HCP) are often formed in HEA atoms without intermetallics or complex phases [118]. In addition, the excellent electrical conductivity of HEAs can promote electron transfer in the catalysis of HER, and its structural stability also provides a channel for further improving the stability of electro-catalytic materials, making them excellent HER catalysts. In order to further improve the hydrogen evolution electrocatalytic activity of NiMo-based alloy hydrogen evolution electrodes, enhance the hardness, stability and corrosion resistance, some NiMo-based high-entropy alloy hydrogen evolution electrocatalysts were developed on the basis of NiMo alloys and NiMo-based medium-entropy alloys.

In a series of ternary NiMo-based alloys (NiMoCu, NiMoFe, NiMoW, NiMoZn, etc), NiMoFe amorphous alloy is the typical catalyst with the best hydrogen evolution performance and the best stability. Therefore, Fe element is involved in the reported NiMo-based HEA catalysts for HER.

KANG et al [119] prepared bulk $Ni_{20}Fe_{20}Mo_{10}$-$Co_{35}Cr_{15}$ HEAs as noble metal-free electrocatalysts (Figs. 5(a, b)), which exhibited high activity and excellent stability in both acidic and basic solutions, even comparable to commercial Pt/C (Figs. 5(c, d)). Moreover, single-phase HEAs have lower charge transfer resistance compared with biphasic HEAs, which facilitates charge transfer and electron transport during the HER reaction. Notably, the excellent HER activity of $Ni_{20}Fe_{20}Mo_{10}Co_{35}Cr_{15}$ HEAs was measured in bulk samples with lower electrochemically active specific surface areas, but the catalysts with this structure showed poor cycling stability in solution. Therefore, the nano-porous structure of multi-component alloys is an effective strategy to improve the stability of electrocatalysts and enhance the electrocatalytic activity.

QIU et al [120] synthesized three single-phase nanoporous high-entropy alloys (np-HEAs) by combining the alloy melting and rapid cooling methods, in which AlNiCuMoCoFe was dissolved in 0.1 mol/L KOH solution, and showed excellent HER performance. It can be seen from the LSV curve in Fig. 5(f) that the overpotential of the AlNiCuMoCoFe catalyst is significantly lower than

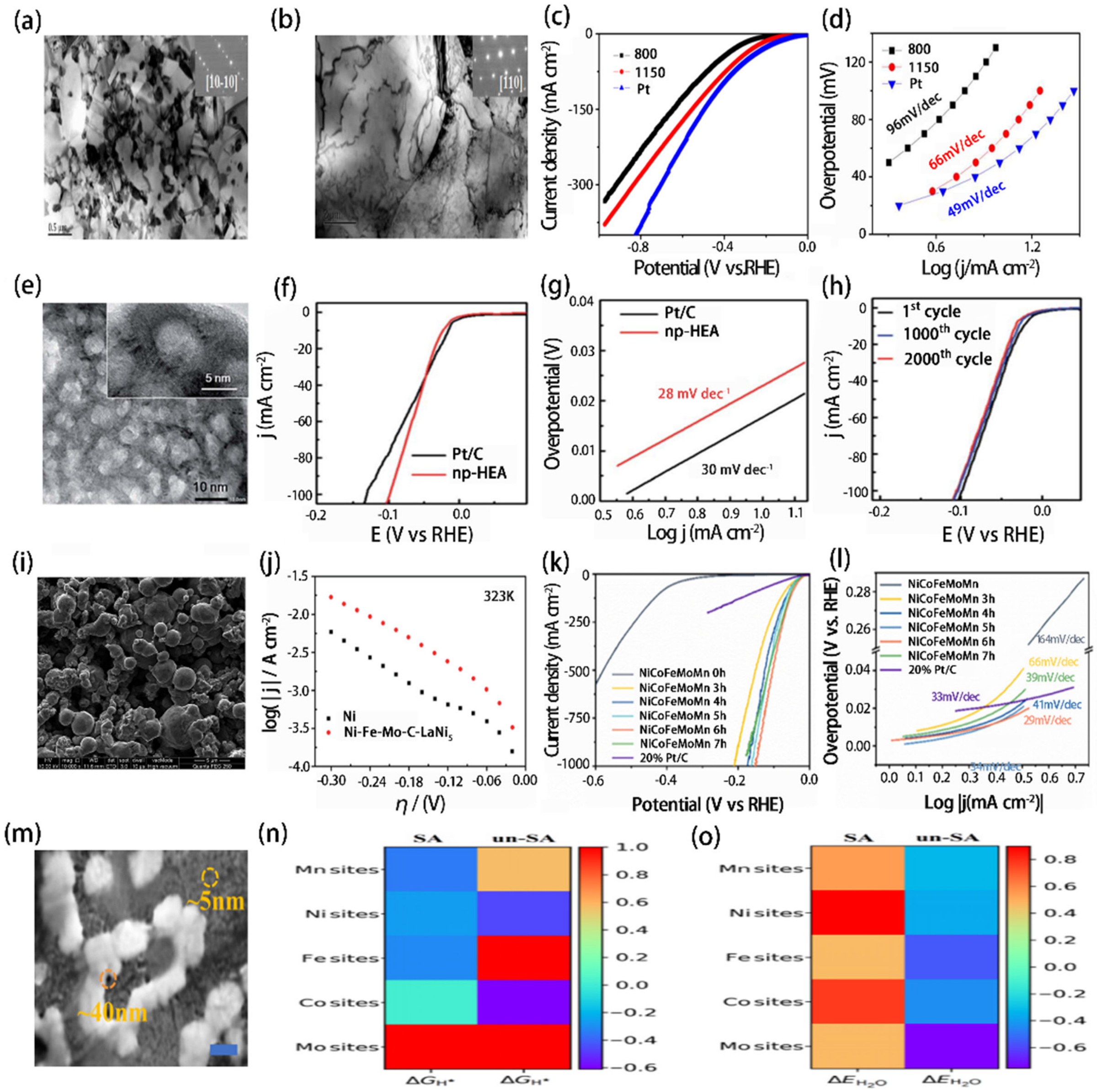

Fig. 5 TEM images of HEAs after annealing at 800 °C (a) and 1150 °C (b) [119]; Polarization curves (c) and Tafel plots of polarization curves (d) of dual-phase, single-phase HEAs and Pt electrodes [119]; TEM image of alloyed hexa-np-HEA [120] (e); Polarization curve of HER (f); Tafel curve (g) and durability test results (h) of np-HEA and Pt/C [120]; SEM image of porous Ni−Fe−Mo−C−LANi$_5$ electrode [122] (i); Linear Tafel polarization recorded on Ni and Ni−Fe−Mo−C−LANi$_5$ electrocatalyst in 6 mol/L KOH solution at 323 K [122] (j); HER polarization curves of NiCoFeMoMn and commercial Pt/C in 1 mol/L KOH solution (scan rate: 1 mV/s) [123] (k); Tafel plots of different electrocatalytic materials [123] (l); SEM image of np-NiCoFeMoMn [123] (m); Colored ΔG_{H^*} comparisons of SA and un-SA [123] (n); Colored $\Delta E_{\mathrm{H_2O}}$ comparisons of SA and un-SA [123] (o)

that of Pt/C. Notably, its Tafel slope is only 28 mV/dec (Fig. 5(g)). This nanoporous structure has bright pores and dark alloy ligaments revealed by TEM image (Fig. 5(e)). Furthermore, np-HEAs are very stable during continuous electrocatalysis with only minor changes after 2000 CV cycles (Fig. 5(h)). Compared with previous bulk multicomponent alloys, the preparation of such nanoscale HEAs is a new breakthrough, and the pore structure with larger pore size facilitates electron transport in electrochemical reactions. The nanoporous CuAlNiMoFe electrode prepared by YAO et al [121] also has excellent electrocatalytic hydrogen evolution performance. The catalyst consists of uniform interpenetrating nanopores and interconnected Cu ligaments. This unique bimodal porous structure facilitates electron transfer along the interconnected Cu ligaments, and the 3D nanoporous Cu framework plays an important role in the high-performance HER electrocatalysis of nanoporous CuAlNiMoFe electrodes. The electrochemical tests show that the electrode has an ultra-small overpotential of 9.7 mV at a current density of 10 mA/cm^2. Meanwhile, the electrochemical active area and charge transfer resistance of the nanoporous CuAlNiMoFe electrode are better than those of other samples, indicating better electrocatalytic activity. In addition, the current density did not change significantly when tested at an overpotential of 50 mV for more than 200 h, and the SEM images were also the same as the initial ones, demonstrating excellent durability. WU et al [122] investigated the HER of Ni−Fe−Mo−C−$LANi_5$ electrodes. The porous microstructure can be clearly seen by the SEM image (Fig. 5(i)). This structure shows that the electrode has a high open porosity, which effectively increases the specific surface area and improves the electrocatalytic hydrogen evolution activity of porous Ni−Fe−Mo−C−$LANi_5$. Figure 5(j) shows a set of Tafel curves for the porous Ni−Fe−Mo−C−$LANi_5$ electrode at 323 K. Compared with pure Ni, Ni alloys with Fe, Mo, C and $LaNi_5$ have higher electrocatalytic performance in HER. This is caused by the synergistic effect between the catalytic properties of Ni and Fe, Mo, and the intercalation of C into the Ni−Fe matrix and the Ni−Fe−Mo matrix, thereby enhancing the intrinsic activity of the material.

The heterostructure-like structure formed by spinodal decomposition of multi-component high-entropy alloys can effectively improve the intrinsic catalytic activity of catalysts. LIU et al [123] first synthesized a novel manganese-rich alloy $Ni_{14}Co_{14}Fe_{14}Mo_6Mn_{52}$ by arc melting and single-roll rapid quenching, and then obtained a hierarchical nanoporous high-entropy NiCoFeMoMn alloy by one-step dealloying. It has excellent HER performance in alkaline solution (Figs. 5(k, l)). Figure 5(m) shows the hierarchical nanoporous structure of NiCoFeMoMn, which can greatly increase the electrochemically active area and expose more electrochemically active sites. Most importantly, the spinodal decomposition of high-entropy alloys leads to the segregation of Mo atoms, and the resulting composition changes provide a richer atomic chemical environment and more active sites for water electrolysis. The DFT results confirm that the heterostructures of element segregation region and non-segregation region synergistically optimize the Gibbs free energy of hydrogen adsorption and H_2O adsorption energy on the active site, reduce the dissociation energy barrier of H_2O, and thus enhance the the intrinsic catalytic activity of the catalyst (Figs. 5(n, o)). Compared with other high-entropy alloys, NiCoFeMoMn can maintain the stability for more than 300 h, and it is a catalyst with good stability at high current density and low potential.

Compared with medium-entropy alloys, the HER performance of NiMo-based high-entropy alloys is improved. Its high HER performance is mainly caused by the synergistic effect among various elements to enhance the intrinsic catalytic activity of the catalyst, as well as to increase the actual surface area. The unique properties and effects of high-entropy alloys are also the main supports as electrocatalysts for hydrogen evolution and they exhibit good HER performance. The HER performance of NiMo-based high-entropy alloy catalysts in alkaline medium is given in Table 3. Electrocatalytic hydrogen evolution performance exhibited by the addition of more new elements is worth expecting. However, the research on HEA electrocatalysts is still in its infancy, and the preparation of HEA nanostructures is also a challenge. With the continuous deepening of research work, these new materials have the potential to play a more important impact in the future field of catalysis.

4 Some key issues

Although the excellent properties of amorphous alloy materials have been widely concerned, the research on water electrolysis is still in its infancy, and there are still some key issues to be solved:

(1) Preparation technology

Due to the continuous change of alloy composition, the synergistic effect between alloys makes it have higher activity and better stability, which requires that its preparation technology should also be improved and innovated. It is our breakthrough direction to directly obtain catalysts with high specific surface area and inherent catalytic activity through a simple preparation process.

Table 3 HER performance of NiMo-based high-entropy alloys

Catalyst	Electrolyte	Overpotential, η_{10}/mV	Tafel slope/(mV·dec^{-1})	Reference
$Ni_{20}Fe_{20}Mo_{10}Co_{35}Cr_{15}$	1 mol/L KOH	172	66	[119]
AlNiCuMoCoFe	0.1 mol/L KOH		28	[120]
CuAlNiMoFe	1 mol/L KOH	9.7	60	[121]
Ni−Fe−Mo−C−$LANi_5$	6 mol/L KOH		140	[122]
NiCoFeMoMn	1 mol/L KOH	150 (η_{1000})	25	[123]

(2) Component regulation

Component regulation is also crucial for the improvement of catalyst performance. Although there are many types of amorphous alloy catalysts, there are few studies on high-entropy alloy catalysts with multiple components. Therefore, in future research, it is possible to try to add a variety of different elements such as transition metals, rare earths, and non-metals to the catalyst, and then explore its catalytic activity and stability. And it is further confirmed that the synergistic mechanism between alloys is one of the main reasons to promote the improvement of catalytic performance.

(3) Nanoscale

Amorphous alloy nanoscale has received extensive attention and has been rapidly developed, but the design of small-scale nanostructured catalysts through a compositionally efficient and environmentally friendly approach is still the focus of our research.

(4) Electronic structure

The control of the electronic structure of the catalyst surface can effectively improve the catalytic performance of the catalyst. Afterwards, surface functionalization methods such as element doping and defect engineering can effectively change the electronic structure of the catalyst, such as electronic states, energy bands, orbitals, and spins, thereby affecting the interfacial charge transfer kinetics, which in turn affects the catalytic performance.

(5) Catalytic mechanism

Although some complex multi-element system (HEAs) catalysts have good electrocatalytic performance, their real catalytic mechanism is still unclear. The identification of active sites helps to clarify the catalytic mechanism. To this end, we can actively try to use X-ray absorption spectroscopy (XAS) and density functional theory (DFT) calculations to identify active sites and clarify the location and type of active sites.

5 Conclusions

Each NiMo-based amorphous alloy catalyst has its own unique structure, surface morphology, and different element contents. Rational regulation of these conditions can increase the specific surface area, the number of active sites, and promote the synergy between elements, which in turn enhances the electrocatalytic hydrogen evolution (HER) performance. An ideal electrocatalyst should have at least the following properties: (1) high electrocatalytic activity, (2) good electronic conductivity, (3) good electrochemical stability and corrosion resistance, and (4) low cost and easy fabrication. In addition to increasing the specific surface area and exposing more active sites, improving the intrinsic activity of the catalyst is also a top priority. The optimization and improvement of the high activity and stability of NiMo-based amorphous alloy catalysts will always be a key research topic for material researchers. It is hoped that the review of NiMo-based amorphous alloys in this work can help to better design NiMo-based amorphous alloys and gain a deeper understanding of the catalytic mechanism of NiMo-based amorphous alloys for HER.

CRediT authorship contribution statement

Si-xuan ZHANG: Conceptualization, Methodology, Formal analysis, Writing − Original draft; **Jin-zhao HUANG:** Supervision, Funding acquisition, Writing − Review & editing; **Dian-jin DING:** Formal analysis, Investigation, Writing − Review & editing; **Jun TANG:** Formal analysis, Investigation, Writing − Review & editing; **Xiao-long DENG:** Supervision, Funding acquisition, Writing − Review & editing.

Declaration of competing interest

The authors declare that they have no known competing financial interests or personal relationships that could have appeared to influence the work reported in this paper.

Acknowledgments

This work was supported by the Introduction and Cultivation Plan of Young Innovative Talents in Colleges and Universities of Shandong Province, China, the Natural Science Foundation of Shandong Province, China (No. ZR2020ME052), the Natural Science Research Fund for Colleges and Universities in Anhui Province, China (No. KJ2021A0387), and Independent Cultivation Program of Innovation Team of Jinan City, China (No. 2019GXRC011).

References

[1] ZHANG Jian, HE Liu, YAO Yuan, ZHOU Xiao-jie, JIANG Li-kun, PENG Ping. Hydrogen storage properties of magnesium hydride catalyzed by Ni-based solid solutions [J]. Transactions of Nonferrous Metals Society of China, 2022, 32: 604−617.

[2] WANG Mei, ZHANG Wen-juan, ZHANG Fang-fang, ZHANG Zhong-hua, TANG Bin, LI Jin-ping, WANG Xiao-guang. Theoretical expectation and experimental implementation of in situ Al-doped CoS_2 nanowires on dealloying-derived nanoporous intermetallic substrate as an efficient electrocatalyst for boosting hydrogen production [J]. ACS Catalysis, 2019, 9: 1489−1502.

[3] WANG Jie, WU Chang-sheng, DAI Ye-jing, ZHAO Zhi-hao, WANG A, ZHANG Tie-jun, WANG Zhong-lin. Achieving ultrahigh triboelectric charge density for efficient energy harvesting [J]. Nature Communications, 2017, 8: 1−8.

[4] LUYEN DOAN T L, TRAN D T, NGUYEN D C, TUAN LE H, KIM N H, LEE J H. Hierarchical three-dimensional framework interface assembled from oxygen-doped cobalt phosphide layer-shelled metal nanowires for efficient electrocatalytic water splitting [J]. Applied Catalysis B: Environmental, 2020, 261: 118268.

[5] CHEN Yan, ZHANG Hao-yu, WU Fu-ying, SUN Ze, ZHENG Jia-guang, ZHANG Liu-ting, CHEN Li-xin. Mn nanoparticles enhanced dehydrogenation and hydrogenation kinetics of MgH_2 for hydrogen storage [J]. Transactions of Nonferrous Metals Society of China, 2021, 31: 3469−3477.

[6] HU Qi, LI Guo-min, HAN Zhen, WANG Zi-yu, HUANG Xiao-wan, YANG Heng-pan, ZHANG Qian-ling, LIU Jian-hong, HE Chuan-xin. Recent progress in the hybrids of transition metals/carbon for electrochemical water splitting [J]. Journal of Materials Chemistry A, 2019, 7: 14380−14390.

[7] SHEN Hui-dong, PEPPEL T, STRUNK J, SUN Zhen-yu. Photocatalytic reduction of CO_2 by metal-free-based materials: Recent advances and future perspective [J]. Solar RRL, 2020, 4: 1900546.

[8] WEI Bei, XU Guan-cheng, HEI Jin-cheng, ZHANG Li, HUANG Ting-ting, WANG Qian. CoFeP hierarchical nanoarrays supported on nitrogen-doped carbon nanofiber as efficient electrocatalyst for water splitting [J]. Journal of Colloid and Interface Science, 2021, 602: 619−626.

[9] TRAN D T, HOA V H, PRABHAKARAN S, KIM D H, KIM N H, LEE J H. Activated CuNi@ Ni Core@ shell structures via oxygen and nitrogen dual coordination assembled on 3D CNTs-graphene hybrid for high-performance water splitting [J]. Applied Catalysis B: Environmental, 2021, 294: 120263.

[10] CHI Jun, YU Hong-mei. Water electrolysis based on renewable energy for hydrogen production [J]. Chinese Journal of Catalysis, 2018, 39: 390−394.

[11] LI Dong-ze, LIU Hui, FENG Li-gang. A review on advanced FeNi-based catalysts for water splitting reaction [J]. Energy & Fuels, 2020, 34: 13491−13522.

[12] ANWAR S, KHAN F, ZHANG Ya-hui, DJIRE A. Recent development in electrocatalysts for hydrogen production through water electrolysis [J]. International Journal of Hydrogen Energy, 2021, 46: 32284−32317.

[13] SANTOS A L, CEBOLA M J, SANTOS D M F. Towards the hydrogen economy — A review of the parameters that influence the efficiency of alkaline water electrolyzers [J]. Energies, 2021, 14: 3193.

[14] TAJUDDIN A A H, ELUMALAI G, XI Ze-yu, HU Kai-long, JEONG S, NAGASAWA K, FUJITA J I, SONE Y, ITO Y. Corrosion-resistant non-noble metal electrodes for PEM-type water electrolyzer [J]. International Journal of Hydrogen Energy, 2021, 46: 38603−38611.

[15] ZHENG Yun, CHEN Zong-wei, Zhang Jiu-jun. Solid oxide electrolysis of H_2O and CO_2 to produce hydrogen and low-carbon fuels [J]. Electrochemical Energy Reviews, 2021, 4: 508−517.

[16] HANSEN J B. Solid oxide electrolysis—A key enabling technology for sustainable energy scenarios [J]. Faraday Discussions, 2015, 182: 9−48.

[17] EBBESEN S D, JENSEN S H, HAUCH A, MOGENSEN M B. High temperature electrolysis in alkaline cells, solid proton conducting cells, and solid oxide cells [J]. Chemical Reviews, 2014, 114: 10697−10734.

[18] MANDAL M. Recent advancement on anion exchange membranes for fuel cell and water electrolysis [J]. ChemElectroChem, 2021, 8: 36−45.

[19] DARBAND G B, ALIOFKHAZRAEI M, ROUHAGHDAM A S, KIANI M A. Three-dimensional Ni−Co alloy hierarchical nanostructure as efficient non-noble-metal electrocatalyst for hydrogen evolution reaction [J]. Applied Surface Science, 2019, 465: 846−862.

[20] JAMEEI RAD P, ALIOFKHAZRAEI M, BARATI DARBAND G. Ni−W nanostructure well-marked by Ni selective etching for enhanced hydrogen evolution reaction [J]. International Journal of Hydrogen Energy, 2019, 44: 880−894.

[21] CURCIO A, WANG Jian, WANG Zheng, ZHANG Zhi-qi, BELOTTI A, PEPE S, EFFAT M B, SHAO Zong-ping, LIM J, CIUCCI F. Unlocking the potential of mechanochemical coupling: Boosting the oxygen evolution reaction by mating proton acceptors with electron donors [J]. Advanced Functional Materials, 2021, 31: 2008077.

[22] LI Feng, HAN Gao-feng, NOH H J, JEON J P, AHMAD I, CHEN Shan-shan, YANG C, BU Yun-fei, FU Zhen-ping, LIU Ya-lin, BAEK J B. Balancing hydrogen adsorption/

desorption by orbital modulation for efficient hydrogen evolution catalysis [J]. Nature Communications, 2019, 10: 1−7.

[23] LIU Bi-tao, WU Cheng-rong, CHEN Gen, CHEN Wen-bo, PENG Ling-ling, YAO Yu-cen, WEI Zhao, ZHU Hong, HAN Tao, TANG Dian-yong, ZHOU Min. All-in-one surface engineering strategy on nickel phosphide arrays towards a robust electrocatalyst for hydrogen evolution reaction [J]. Journal of Power Sources, 2019, 429: 46−54.

[24] ITO Y, OHTO T, HOJO D, WAKISAKA M, NAGATA Y, CHEN Ling-han, HU Kai-long, IZUMI M, FUJITA J I, ADSCHIRI T. Cooperation between holey graphene and NiMo alloy for hydrogen evolution in an acidic electrolyte [J]. ACS Catalysis, 2018, 8: 3579−3586.

[25] ZHANG Jian, WANG Tao, LIU Pan, LIAO Zhong-quan, LIU Shao-hua, ZHUANG Xiao-dong, CHEN Ming-wei, ZSCHECH E, FENG Xin-liang. Efficient hydrogen production on $MoNi_4$ electrocatalysts with fast water dissociation kinetics [J]. Nature Communications, 2017, 8: 1−8.

[26] ZHOU Yu-xue, LUO Min, ZHANG Wei, ZHANG Zhen-xin, MENG Xiang-dong, SHEN Xiao-shuang, LIU Hong-fei, ZHOU Min, ZENG Xiao-hua. Topological formation of a Mo–Ni-based hollow structure as a highly efficient electrocatalyst for the hydrogen evolution reaction in alkaline solutions [J]. ACS Applied Materials & Interfaces, 2019, 11: 21998−22004.

[27] DAI Chun-ke, FU Yu, PAN Yue, YIN Yu-peng, DU Cui-wei, LIU Zhi-yong. Microstructure and mechanical properties of $FeCoCrNiMo_{0.1}$ high-entropy alloy with various annealing treatments [J]. Materials Characterization, 2021, 179: 111313.

[28] TANG Jian, XU Ji-lin, LI Liang-liang, MA Yong-cun, YE Zhi-guo, LUO Hong-yu, LUO Jun-ming. In-situ hydrothermal synthesis of Ni−MoO_2 heterostructure on porous bulk NiMo alloy for efficient hydrogen evolution reaction [J]. Transactions of Nonferrous Metals Society of China, 2022, 32: 1598−1608.

[29] TOMBOC G M, KWON T, JOO J, LEE K. High entropy alloy electrocatalysts: A critical assessment of fabrication and performance [J]. Journal of Materials Chemistry A, 2020, 8: 14844−14862.

[30] FENG Jun-jie, GAO Shuo, HAN Kun, MIAO Yi-dong, QI Ji-qiu, WEI Fu-xiang, REN Yao-jian, ZHAN Zhen-zhen, SUI Yan-wei, SUN Zhi, CAO Peng. Effects of minor B addition on microstructure and properties of $Al_{19}Co_{20}Fe_{20}Ni_{41}$ eutectic high-entropy alloy [J]. Transactions of Nonferrous Metals Society of China, 2021, 31: 1049−1058.

[31] KLEMENT W, WILLENS R H, DUWEZ P. Non-crystalline structure in solidified gold–silicon alloys [J]. Nature, 1960, 187: 869−870.

[32] ZHAO C C, INOUE A, KONG F L, ZHANG J Y, CHEN C J, SHEN B L, AL-MARZOUKI F, GREER A L. Novel phase decomposition, good soft-magnetic and mechanical properties for high-entropy $(Fe_{0.25}Co_{0.25}Ni_{0.25}Cr_{0.125}Mn_{0.125})_{100-x}B_x$ (x=9−13) amorphous alloys [J]. Journal of Alloys and Compounds, 2020, 843: 155917.

[33] SILVEYRA J M, FERRARA E, HUBER D, MONSON T. Soft magnetic materials for a sustainable and electrified world [J]. Science, 2018, 362: eaao0195.

[34] DONG Chuang, WANG Zi-jian, ZHANG Shuang, WANG Ying-min. Review of structural models for the compositional interpretation of metallic glasses [J]. International Materials Reviews, 2020, 65: 286−296.

[35] LI Xing-yun, CAI Wei-zheng, LI Dong-sheng, XU Jun, TAO Hua-bing, LIU Bin. Amorphous alloys for electrocatalysis: The significant role of the amorphous alloy structure [J]. Nano Research, 2023, 16: 4277−4288.

[36] SUN B A, WANG W H. The fracture of bulk metallic glasses [J]. Progress in Materials Science, 2015, 74: 211−307.

[37] ZHU Fan, SONG Shuang-xi, REDDY K M, HIRATA A, CHEN Ming-wei. Spatial heterogeneity as the structure feature for structure–property relationship of metallic glasses [J]. Nature Communications, 2018, 9: 3965.

[38] PEI Chao-qun, CHEN Shuang-qin, ZHAO Tian-chen, LI Mai, CUI Zhao-tao, SUN Bao-an, HU Si-gui, LAN Si, HAHN H, FENG Tao. Nanostructured metallic glass in a highly upgraded energy state contributing to efficient catalytic performance [J]. Advanced Materials, 2022, 34: 2200850.

[39] FENG Guang, NING Fang-hua, SONG Jin, SHANG Huai-fang, ZHANG Kun, DING Zheng-ping, GAO Peng, CHU Wang-sheng, XIA Ding-guo. Sub-2 nm ultrasmall high-entropy alloy nanoparticles for extremely superior electrocatalytic hydrogen evolution [J]. Journal of the American Chemical Society, 2021, 143: 17117−17127.

[40] SMITH G V, BROWER W E, MATYJASZCZYK M S, PETTIT T L. Metallic glasses: New catalyst systems [M]// New Horizons in Catalysis, Proceedings of the 7th International Congress on Catalysis. Amsterdam: Elsevier, 1981: 355−363.

[41] ZHANG Sai, XIA Zhao-ming, NI Ting, ZHANG Huan, WU Chao, QU Yong-quan. Tuning chemical compositions of bimetallic AuPd catalysts for selective catalytic hydrogenation of halogenated quinolines [J]. Journal of Materials Chemistry A, 2017, 5: 3260−3266.

[42] YUAN Lin-shan, ZHENG Yi-xiong, JIA Meng-lu, ZHANG Shu-jin, WANG Xiu-lin, PENG Cheng. Nanoporous nickel-copper-phosphorus amorphous alloy film for methanol electro-oxidation in alkaline medium [J]. Electrochimica Acta, 2015, 154: 54−62.

[43] ZHANG Shu-jin, ZHENG Yi-xiong, YUAN Lin-shan, ZHAO Li-hua. Ni−B amorphous alloy nanoparticles modified nanoporous Cu toward ethanol oxidation in alkaline medium [J]. Journal of Power Sources, 2014, 247: 428−436.

[44] ZHANG Shu-jin, ZHENG Yi-xiong, YUAN Lin-shan, WANG X L, ZHAO Li-hua. In situ synthesis of nickel–boron amorphous alloy nanoparticles electrode on nanoporous copper film/brass plate for ethanol electro-oxidation [J]. International Journal of Hydrogen Energy, 2014, 39: 3100−3108.

[45] WU Fan-hua, ZHANG Zhong-lin, ZHANG Fu-sheng, DUAN Dong-hong, LI Yu, WEI Guo-qiang, LIU Shi-bin, YUAN Qin-bo, WANG En-zhi, HAO Xiao-gang. Exploring the role of cobalt in promoting the electroactivity of amorphous Ni−B nanoparticles toward methanol oxidation [J]. Electrochimica Acta, 2018, 287: 115−123.

[46] WU Fan-hua, ZHANG Zhong-lin, ZHANG Fu-sheng,

DUAN Dong-hong, LI Yu, WEI Guo-qiang, LIU Shi-bin, YUAN Qin-bo, WANG En-zhi, HAO Xiao-gang. New insights into the electrocatalytic mechanism of methanol oxidation on amorphous Ni−B−Co nanoparticles in alkaline media [J]. Catalysts, 2019, 9: 749.

[47] MA Pei-yan, ZHAO Ming-ming, ZHANG Long, WANG Heng, GU Jun-feng, SUN Yu-chen, JI Wei, FU Zheng-yi. Self-supported high-entropy alloy electrocatalyst for highly efficient H_2 evolution in acid condition [J]. Journal of Materiomics, 2020, 6: 736−742.

[48] LI Rui, LIU Xiong-jun, WU Ruo-yu, WANG Jing, LI Zhi-bin, CHAN K C, WANG Hui, WU Yan, LU Zhao-ping. Flexible honeycombed nanoporous/glassy hybrid for efficient electrocatalytic hydrogen generation [J]. Advanced Materials, 2019, 31: 1904989.

[49] CHU Fei, HAN Bin, EDALATI K, MA Jiang, MENG Yu-ying, WANG Chao, YANG Fan, ZHANG Peng, LIN Huai-jun. Severe plastic deformed Pd-based metallic glass for superior hydrogen evolution in both acidic and alkaline media [J]. Scripta Materialia, 2021, 204: 114145.

[50] BROWER W E Jr, MATYJASZCZYK M S, PETTIT T L, SMITH G V. Metallic glasses as novel catalysts [J]. Nature, 1983, 301: 497−499.

[51] SI Chao-run, ZHANG Zi-qian, ZHANG Qi, CAI Jin. Influence of mechanical alloying on the particle size, microstructure and soft magnetic properties of coarse Fe-based amorphous powders prepared by gas atomization [J]. Journal of Non-Crystalline Solids, 2021, 559: 120675.

[52] GUTPA J, SHAIK H, NAVEEN KUMAR K, SATTAR S A. PVD techniques proffering avenues for fabrication of porous tungsten oxide (WO_3) thin films: A review [J]. Materials Science in Semiconductor Processing, 2022, 143: 106534.

[53] DENG Y, CHEN Wang-lin, LI Bing-xin, WANG Cheng-yong, KUANG Tong-chun, LI Yan-qiu. Physical vapor deposition technology for coated cutting tools: A review [J]. Ceramics International, 2020, 46: 18373−18390.

[54] BAPTISTA A, SILVA F J G, PORTEIRO J, MÍQUEZ J L, PINTO G, FERNANDES L. On the physical vapour deposition (PVD): Evolution of magnetron sputtering processes for industrial applications [J]. Procedia Manufacturing, 2018, 17: 746−757.

[55] XIN Yue, LI Shu-hui, QIAN Ya-yang, ZHU Wen-kun, YUAN Hai-bo, JIANG Peng-yan, GUO Rui-han, WANG Liang-bing. High-entropy alloys as a platform for catalysis: Progress, challenges, and opportunities [J]. ACS Catalysis, 2020, 10: 11280−11306.

[56] LI Jin-yang, DOUBEK G, MCMILLON-BROWN L, TAYLOR A D. Recent advances in metallic glass nanostructures: Synthesis strategies and electrocatalytic applications [J]. Advanced Materials, 2019, 31: 1802120.

[57] ZHANG Jing, WANG Fan, SHENOY V B, TANG Ming, LOU Jun. Towards controlled synthesis of 2D crystals by chemical vapor deposition (CVD) [J]. Materials Today, 2020, 40: 132−139.

[58] XIA Z H, ZHANG M, ZHANG Y, ZHAO Y, LIAW P K, QIAO J W. Effects of Ni−P amorphous films on mechanical and corrosion properties of $Al_{0.3}CoCrFeNi$ high-entropy alloys [J]. Intermetallics, 2018, 94: 65−72.

[59] KALE M B, BORSE R A, GOMAA ABDELKADER MOHAMED A, WANG Yao-bing. Electrocatalysts by electrodeposition: Recent advances, synthesis methods, and applications in energy conversion [J]. Advanced Functional Materials, 2021, 31: 2101313.

[60] FANG Ming, DONG Guo-fa, WEI Ren-jie, HO J C. Hierarchical nanostructures: Design for sustainable water splitting [J]. Advanced Energy Materials, 2017, 7: 1700559.

[61] WANG Zi-jian, LI Ming-xing, YU Ji-hao, GE Xing-bo, LIU Yan-hui, WANG Wei-hua. Low-iridium-content IrNiTa metallic glass films as intrinsically active catalysts for hydrogen evolution reaction [J]. Advanced Materials, 2020, 32: 1906384.

[62] XUE Ming-ming, MAO Xing-ye, LV Yi-lin, CHI Yun-long, YANG Yong, HE Ji-ning, DONG Yan-chun. Comparison of micro-nano FeCoNiCrAl and FeCoNiCrMn coatings prepared from mechanical alloyed high-entropy alloy powders [J]. Journal of Thermal Spray Technology, 2021, 30: 1666−1678.

[63] SURYANAARAYANA C. Mechanical alloying: A novel technique to synthesize advanced materials [J]. Research, 2019, 2019.

[64] CAO Yan-peng, CHEN Zhi-chao, YE Feng, YANG Ya-kun, WANG Kai-chen, WANG Zhi-ming, YIN Li-kun, XU Chao. One-step synthesis of amorphous NiCoP nanoparticles by electrodeposition as highly efficient electrocatalyst for hydrogen evolution reaction in alkaline solution [J]. Journal of Alloys and Compounds, 2022, 896: 163103.

[65] HUANG De-kang, LI Shu, LUO Yan-zhu, LIAO Li, YE Jin-hua, CHEN Hao. Self-templated construction of 1D NiMo nanowires via a Li electrochemical tuning method for the hydrogen evolution reaction [J]. Nanoscale, 2019, 11: 19429−19436.

[66] NAIRAN A, ZOU Pei-chao, LIANG Cai-wu, LIU Jia-xing, WU Dang, LIU Peng, YANG Cheng. NiMo solid solution nanowire array electrodes for highly efficient hydrogen evolution reaction [J]. Advanced Functional Materials, 2019, 29: 1903747.

[67] SHANG Peng-fei, YE Zhi-guo, DING Yi, ZHU Zhi-xiang, PENG Xin-yuan, MA Guang, LI Duo-sheng. Nanosponge-like solid solution of NiMo with a high hydrogen evolution reaction performance over a wide range of current densities [J]. ACS Sustainable Chemistry & Engineering, 2020, 8: 10664−10672

[68] YANG Pan, YUE Chun-hui, YANG Ying-nan, WANG Jing-chuan, HAO Ya-wei, HUANG He-shun, ZHU Jing, YUE Guo-zong, ZHANG Xiao-chong, YANG Li-jun. Electrospun NiMo nanobelts self-supported electrodes for efficient hydrogen evolution reaction in alkaline media [J]. Chemical Physics Letters, 2021, 770: 138341.

[69] ZHANG Dang-quan, ASHRAF M A. Electrochemical fabrication of Ni−Mo nanostars with Pt-like catalytic activity for both electrochemical hydrogen and oxygen evolution reactions [J]. International Journal of Hydrogen Energy, 2020, 45: 30533−30546.

[70] SAJJAD S, WANG Chao, WANG Xian-fu, ALI T, QIAN Tao, YAN Cheng-lin. In situ evolved NiMo/$NiMoO_4$ nanorods as a bifunctional catalyst for overall water splitting [J]. Nanotechnology, 2020, 31: 495404.

[71] ZHANG Ji-tang, GUO Shuai, XIAO Bei-bei, LIN Zhi-ping,

YAN Ling-hui, DU Da-min, SHEN Shi-jie. Ni-Mo based mixed-phase polyionic compounds nanorod arrays on nickel foam as advanced bifunctional electrocatalysts for water splitting [J]. Chemical Engineering Journal, 2021, 416: 129127.

[72] XU J L, LI L L, TANG J, DAI L, LI X B, YE Z G, LUO J M. Powder metallurgy synthesis of porous NiMo alloys as efficient electrocatalysts to enhance the hydrogen evolution reaction [J]. Journal of Alloys and Compounds, 2021, 865: 158901.

[73] BENAVENTE LLORENTE V, DIAZ L A, LACCONI G I, ABUIN G C, FRANCESCHINI E A. Effect of duty cycle on NiMo alloys prepared by pulsed electrodeposition for hydrogen evolution reaction [J]. Journal of Alloys and Compounds, 2022, 897: 163161.

[74] ZU Li-guo, HE Jia-huan, LIU Xin-li, ZHANG Lei, ZHOU Ke-chao. Effect of pore orientation on the catalytic performance of porous NiMo electrode for hydrogen evolution in alkaline solutions [J]. International Journal of Hydrogen Energy, 2019, 44: 4650−4655.

[75] ZHU Yin-an, PAN Ye, DAI Wei-ji, LU Tao. Dealloying generation of oxygen vacancies in the amorphous nanoporous Ni−Mo−O for superior electrocatalytic hydrogen generation [J]. ACS Applied Energy Materials, 2020, 3: 1319−1327.

[76] GAO Wei, GOU Wang-yan, ZHOU Xue-mei, HO J C, MA Yuan-yuan, QU Yong-quan. Amine-modulated/engineered interfaces of NiMo electrocatalysts for improved hydrogen evolution reaction in alkaline solutions [J]. ACS Applied Materials & Interfaces, 2018, 10: 1728−1733.

[77] SUN Jia-meng, YU Bin, TAN Fu-quan, YANG Wan-fang, CHENG Guan-hua, ZHANG Zhong-hua. High throughput preparation of Ni−Mo alloy thin films as efficient bifunctional electrocatalysts for water splitting [J]. International Journal of Hydrogen Energy, 2022, 47: 15764−15774.

[78] YUAN Wen-jin, CUI Zhen-duo, ZHU Sheng-li, LI Zhao-yang, WU shui-lin, LIANG Yan-qin. Structure engineering of electrodeposited NiMo films for highly efficient and durable seawater splitting [J]. Electrochimica Acta, 2021, 365: 137366.

[79] YU Xiang-tao, WANG Ming-yong, WANG Zhi, GONG Xu-zhong, GUO Zhan-cheng. Time-dependent surface structure evolution of NiMo films electrodeposited under super gravity field as electrocatalyst for hydrogen evolution reaction [J]. The Journal of Physical Chemistry C, 2017, 121: 16792−16802.

[80] YUAN Fu-hang, MOHAMMADI M R, MA Li-li, CUI Zhen-duo, ZHU Sheng-li, LI Zhao-yang, WU Shui-lin, JIANG Hui, LIANG Yan-qin. Electrodeposition of self-supported NiMo amorphous coating as an efficient and stable catalyst for hydrogen evolution reaction [J]. Rare Metals, 2022, 41: 2624−2632.

[81] PANDA C, MENEZES P W, YAO Sheng-lai, SCHMIDT J, WALTER C, HAUSMANN J N, DRIESS M. Boosting electrocatalytic hydrogen evolution activity with a $NiPt_3$@NiS heteronanostructure evolved from a molecular nickel–platinum precursor [J]. Journal of the American Chemical Society, 2019, 141: 13306−13310.

[82] WANG Shan-shan, XU Ying-chun, FU Ru-ru, ZHU Huan-huan, JIAO Qing-ze, FENG Tong-ying, FENG Cai-hong, SHI Da-xin, LI Han-sheng, ZHAO Yun. Rational construction of hierarchically porous Fe−Co/N-doped carbon/rGO composites for broadband microwave absorption [J]. Nano−Micro Letters, 2019, 11: 1−16.

[83] CHEN Hua-ping, QIAO Shi-zhang, YANG Jing, DU Xi-wen. NiMo/$NiCo_2O_4$ as synergy catalyst supported on nickel foam for efficient overall water splitting [J]. Molecular Catalysis, 2022, 518: 112086.

[84] DENG Shao-feng, LIU Xu-po, HUANG Ting, ZHAO Tong-hui, LU Yun, CHENG Jing-yu, SHEN Tao, LIANG Jia-ning, WANG De-li. MoO_2 modulated electrocatalytic properties of Ni: Investigate from hydrogen oxidation reaction to hydrogen evolution reaction [J]. Electrochimica Acta, 2019, 324: 134892.

[85] WANG Ben-zhi, HUANG He-xiu, HUANG Mei-lin, YAN Pu-xuan, ISIMJAN T T, YANG Xiu-lin. Electron-transfer enhanced MoO_2−Ni heterostructures as a highly efficient pH-universal catalyst for hydrogen evolution [J]. Science China Chemistry, 2020, 63: 841−849.

[86] QIAN Guang-fu, CHEN Jin-lin, YU Tian-qi, LIU Jia-cheng, LUO Lin, YIN Shi-bin. Three-phase heterojunction NiMo-based nano-needle for water splitting at industrial alkaline condition [J]. Nano-Micro Letters, 2022, 14: 1−15.

[87] ZHOU Tao, HUANG Yang-qi, ALI A, PEI K S. Ni-MoO_2 nanoparticles heterojunction loaded on stereotaxically-constructed graphene for high-efficiency overall water splitting [J]. Journal of Electroanalytical Chemistry, 2021, 897: 115555.

[88] CAO Jun, LI Hai-chao, PU Jia-xuan, ZENG Si-chao, LIU Li-mei, ZHANG Long, LUO Feng-hua, MA Li, ZHOU Ke-chao, WEI Qiu-ping. Hierarchical NiMo alloy microtubes on nickel foam as an efficient electrocatalyst for hydrogen evolution reaction [J]. International Journal of Hydrogen Energy, 2019, 44: 24712−24718.

[89] ABUIN G, COPPOLA R, DIAZ L. Ni−Mo alloy electrodeposited over Ni substrate for HER on water electrolysis [J]. Electrocatalysis, 2019, 10: 17−28.

[90] ZHAO Shu-nan, HUANG Jian-fei, LIU Yan-yan, SHEN Jian-hua, WANG Hao, YANG Xiao-ling, ZHU Yi-hua, LI Chun-zhong. Multimetallic Ni−Mo/Cu nanowires as nonprecious and efficient full water splitting catalyst [J]. Journal of Materials Chemistry A, 2017, 5: 4207−4214.

[91] SHETTY S, SADIQ M M J, BHAT D K, HEGDE A C. Electrodeposition of Ni−Mo−rGO composite electrodes for efficient hydrogen production in an alkaline medium [J]. New Journal of Chemistry, 2018, 42: 4661−4669.

[92] HOU Jun-gang, WU Yun-zhen, ZHANG Bo, CAO Shu-yan, LI Zhu-wei, SUN Li-cheng. Rational design of nanoarray architectures for electrocatalytic water splitting [J]. Advanced Functional Materials, 2019, 29: 1808367.

[93] WENG Chuan-xin, DAI Zhao-he, WANG Guo-rui, LIU Lu-qi, ZHANG Zhong. Elastomer-free, stretchable, and conformable silver nanowire conductors enabled by three-dimensional buckled microstructures [J]. ACS Applied Materials & Interfaces, 2019, 11: 6541−6549.

[94] LIU Ya, TANG Wen-zhu, ZHANG Gao-wei, CHEN Wen-hao, CHEN Qing-ze, XIAO Chun-lin, XIE Sheng-hui,

QIU Y J. A 3D binder-free AgNWs@ NiMo/PU electrode for efficient hydrogen evolution reaction [J]. Journal of Electroanalytical Chemistry, 2021, 886: 115136.

[95] GÓMEZ M J, DIAZ L A, FRANCESCHINI E A, LACCONI G I, ABUIN G C. 3D nanostructured NiMo catalyst electrodeposited on 316L stainless steel for hydrogen generation in industrial applications [J]. Journal of Applied Electrochemistry, 2019, 49: 1227−1238.

[96] ZHOU Ling-ling, WANG Qi, WANG Jing, CHEN Xue-fei, JIANG Ping, ZHOU Hao, YUAN Fu-ping, XU Xiao-lei, CHENG Zhi-ying, MA En. Atomic-scale evidence of chemical short-range order in CrCoNi medium-entropy alloy [J]. Acta Materialia, 2022, 224: 117490.

[97] ZENG Long-fei, YOU Chao-ping, CAI Xu-feng, WANG Chun-ming, ZHANG Xue-hui, LIANG Tong-xiang. Preparation of nanoporous CoCr alloy by dealloying CrCoNi medium entropy alloys [J]. Journal of Materials Research and Technology, 2020, 9: 6909−6915.

[98] ZHANG Wen-juan, ZHENG Jian, GU Xun-di, TANG Bin, LI Jin-ping, WANG Xiao-guang. Facile synthesis, characterization and DFT studies of a nanostructured nickel–molybdenum–phosphorous planar electrode as an active electrocatalyst for the hydrogen evolution reaction [J]. Nanoscale, 2019, 11: 9353−9361.

[99] ZHANG Ling, WANG Xing-yue, ZHENG Xing-qun, PENG Li-shan, SHEN Jing-jun, XIANG Rui, DENG Zi-hua, LI Li, CHEN Hong-mei, WEI Zi-dong. Oxygen-incorporated $NiMoP_2$ nanowire arrays for enhanced hydrogen evolution activity in alkaline solution [J]. ACS Applied Energy Materials, 2018, 1: 5482−5489.

[100] JEGHAN S M N, KIM N, LEE G. Mo-incorporated three-dimensional hierarchical ternary nickel-cobalt-molybdenum layer double hydroxide for high-efficiency water splitting [J]. International Journal of Hydrogen Energy, 2021, 46: 22463−22477.

[101] HU Kai-long, WU Ming-xing, HINOKUMA S, OHTO T, WAKISAKA M, FUJITA J I, ITO Y. Boosting electrochemical water splitting via ternary NiMoCo hybrid nanowire arrays [J]. Journal of Materials Chemistry A, 2019, 7: 2156−2164.

[102] ZHANG Yong-qi, OUYANG Bo, XU Jing, CHEN Shi, RAWAT R S, FAN Hong-jin. 3D porous hierarchical nickel–molybdenum nitrides synthesized by RF plasma as highly active and stable hydrogen-evolution-reaction electrocatalysts [J]. Advanced Energy Materials, 2016, 6: 1600221.

[103] LASZCZYŃSKA A, SZCZYGIEŁ I. Electrocatalytic activity for the hydrogen evolution of the electrodeposited Co−Ni−Mo, Co−Ni and Co−Mo alloy coatings [J]. International Journal of Hydrogen Energy, 2020, 45: 508−520.

[104] YAN Kai-li, QIN Jun-feng, LIU Zi-zhang, DONG Bin, CHI Jing-qi, GAO Wen-kun, LIN Jia-hui, CHAI Yong-ming, LIU Chen-guang. Organic-inorganic hybrids-directed ternary NiFeMoS anemone-like nanorods with scaly surface supported on nickel foam for efficient overall water splitting [J]. Chemical Engineering Journal, 2018, 334: 922−931.

[105] RASHIDI S, ESFAHANI J A, KARIMI N. Porous materials in building energy technologies — A review of the applications, modelling and experiments [J]. Renewable and Sustainable Energy Reviews, 2018, 91: 229−247.

[106] PANEK J, KUBISZTAL J, BIERSKA-PIECH B. $Ni_{50}Mo_{40}Ti_{10}$ alloy prepared by mechanical alloying as electroactive material for hydrogen evolution reaction [J]. Surface and Interface Analysis, 2014, 46: 716−720.

[107] XIA Ming, LEI Ting, LV Ning-lei, LI Nian-feng. Synthesis and electrocatalytic hydrogen evolution performance of Ni−Mo−Cu alloy coating electrode [J]. International Journal of Hydrogen Energy, 2014, 39: 4794−4802.

[108] YAO Yue, HU En-lai, WANG Zhi-yu, CUI Yuan-jing, QIAN Guo-dong. Boosting hydrogen evolution through the interface effects of amorphous $NiMoO_4$−MoO_2 and crystalline Cu [J]. ACS Omega, 2022, 7: 2244−2251.

[109] TOGHRAEI A, SHAHRABI T, BARATI DARBAND G. Electrodeposition of self-supported Ni−Mo−P film on Ni foam as an affordable and high-performance electrocatalyst toward hydrogen evolution reaction [J]. Electrochimica Acta, 2020, 335: 135643.

[110] BADRNEZHAD R, NASRI F, POURFARZAD H, JAFARI S K. Effect of iron on Ni−Mo−Fe composite as a low-cost bifunctional electrocatalyst for overall water splitting [J]. International Journal of Hydrogen Energy, 2021, 46: 3821−3832.

[111] ABHILASH S, SUMI V S, SARIKA S, DEEPA J P, SREEKALA C O, RIJITH S. Development and characterization of NiMoP alloy coating for electrocatalytic hydrogen evolution reaction in alkaline media [J]. Fuel, 2022, 318: 123598.

[112] LASZCZYŃSKA A, TYLUS W, SZCZYGIEŁ I. Electrocatalytic properties for the hydrogen evolution of the electrodeposited Ni−Mo/WC composites [J]. International Journal of Hydrogen Energy, 2021, 46: 22813−22831

[113] LIU Peng, PAN Wei-sheng, YAO Rui, ZHANG Li-han, WU Qian-yuan, KANG Fei-yu, FAN Hong-jin, YANG Cheng. NiMoFe nanoparticles@ MoO_2 nano-pillar arrays as bifunctional electrodes for ultra-low-voltage overall water splitting [J]. Journal of Materials Chemistry A, 2022, 10: 3760−3770.

[114] WANG Fang-fang, ZHANG Kuan-jian, ZHA Qing-qing, NI Yong-hong. Honeycomb-like Ni−Mo−S on Ni foam as superior bifunctional electrocatalyst for hydrogen evolution and urea oxidation [J]. Journal of Alloys and Compounds, 2022, 899: 163346.

[115] IM H S, PARK S H, HA H J, LEE S M, HEO S, IM S W, NAM K T, LIM S Y. Fabrication of Ni−Mo-based electrocatalysts by modified Zn phosphating for hydrogen evolution reaction [J]. Journal of Electrochemical Science and Technology, 2022, 13: 54−62.

[116] ROS C, MURCIA-LÓPEZ S, GARCIA X, ROSADO M, ARBIOL P J, LLORCA P J, MORANTE P J R. Facing seawater splitting challenges by regeneration with Ni−Mo−Fe bifunctional electrocatalyst for hydrogen and oxygen evolution [J]. ChemSusChem, 2021, 14: 2872−2881.

[117] HEDYA S, MOHAMED L, GABER G, ELKADY O, MEGAHED H, ABOLKASSEM S. Effect of Si/Ti additions on physico-mechanical and chemical properties of FeNiCrCo high entropy alloys manufactured by powder metallurgy technique [J]. Transactions of Nonferrous Metals Society of China, 2022, 32: 2648−2664.

[118] ZHANG Yi-yong, ZHANG Zhi-bin, WANG Xin, YAO Wen, LIANG Xiu-bing. Structure and properties of high-entropy amorphous thin films: A review [J]. JOM, 2022, 74: 794−807.
[119] ZHANG Guo-liang, MING Kai-sheng, KANG Jian-li, HUANG Qin, ZHANG Zhi-jia, ZHENG Xue-rong, BI Xiao-fang. High entropy alloy as a highly active and stable electrocatalyst for hydrogen evolution reaction [J]. Electrochimica Acta, 2018, 279: 19−23.
[120] QIU Hua-jun, FANG Gang, WEN Yu-ren, LIU Pan, XIE Guo-qiang, LIU Xing-jun, SUN Shu-hui. Nanoporous high-entropy alloys for highly stable and efficient catalysts [J]. Journal of Materials Chemistry A, 2019, 7: 6499−6506.
[121] YAO Rui-qi, ZHOU Yi-tong, SHI Hang, WAN Wu-bin, ZHANG Qing-hua, GU Lin, ZHU Yong-fu, WEN Zi, LANG Xing-you, JIANG Qing. Nanoporous surface high-entropy alloys as highly efficient multisite electrocatalysts for nonacidic hydrogen evolution reaction [J]. Advanced Functional Materials, 2021, 31: 2009613.
[122] WU Liang, GUO Xiao-hua, XU Yang, XIAO Yi-feng, QIAN Jin-wen, XU Yan-fei, GUAN Zhuo, HE Yue-hui, ZENG Yi. Electrocatalytic activity of porous Ni−Fe−Mo−C−$LaNi_5$ sintered electrodes for hydrogen evolution reaction in alkaline solution [J]. RSC Advances, 2017, 7: 32264−32274.
[123] LIU Hao, QIN Hong-ye, KANG Jian-li, MA Li-ying, CHEN Guo-xin, HUANG Qin, ZHANG Zhi-jia, LIU En-zuo, LU Huan-ming, LI Jian-xin, ZHAO Nai-qin. A freestanding nanoporous NiCoFeMoMn high-entropy alloy as an efficient electrocatalyst for rapid water splitting [J]. Chemical Engineering Journal, 2022, 435: 134898.

NiMo 基非晶合金电催化析氢反应的进展

张思璇[1]，黄金昭[1]，丁殿金[1]，汤 军[1]，邓小龙[2]

1. 济南大学 物理科学与技术学院，济南 250022；
2. 安徽工业大学 数学与物理学院，马鞍山 243032

摘 要：电催化水分解产生绿色氢气是发展可持续能源体系的重要途径之一。由过渡金属 Ni、Mo 组成的具有高活性、低成本的非晶态合金被广泛认为是一种有效的制氢催化剂。重点关注以镍钼(NiMo)基非晶合金为代表的催化剂，总结非晶态合金的制备方法及其在催化领域的应用，分别叙述 NiMo 合金、NiMo 基中熵合金和 NiMo 基高熵合金在电催化析氢反应(HER)中的应用。结果表明，在合理的功能导向设计下，通过对关键科学及技术问题的解决，NiMo 基非晶态合金催化剂能够表现出良好的析氢性能，最后提出在制备技术、组分调控、纳米化、电子结构以及活化机理 5 个方面还有待解决的问题。这对于催化剂的设计、制备、构效关系及催化机理的研究具有一定的参考价值。

关键词：NiMo 合金；非晶合金；水电解；析氢反应

(Edited by Bing YANG)